FACULTY OF SCIENCE AND TECHNOLOGY

BACHELOR THESIS

Study programme / specialisation:

Mechanical Engineer

The spring semester, 2022

Open

Author:
Mika Tobias Gooding,

Joar Njærheim

Course coordinator:
Knut Erik Teigen Giljarhus

Supervisor(s):
Knut Erik Teigen Giljarhus

Thesis title:

Experimental testing and validation of a disc golf trajectory simulation model

Credits (ECTS): 20

Keywords: Disc golf, full range trajectory, hyzer, anhyzer, flat, Tracker, RHBH, simulation.

Pages: 44

+ **appendix:** 6

Stavanger, 15.05.2022

Summary

The thesis objective is to experimentally test and validate a mathematical model that simulates the trajectory of a thrown golf disc. A number of studies have been conducted with similar thesis statements, but not of a full range trajectory throw. Therefore, one of the main achievements of our study is the method created to perform and analyze these experiments.

The method consisted of developing an experimental setup capable of capturing all parameters that the mathematical model needed to simulate a trajectory. Next, we created a systematic plan of action which would then be used to extract the actual parameters from our experimental footage.

We conducted a study of three different release angles: hyzer, flat and anhyzer. We studied their simulated trajectories and compared them to the actual open environment throws.

Our results showed that the model was capable of producing trajectories similar to open environment throws. At the same time, when comparing the simulated trajectories with the actual throws, the model proved to be sensitive to small changes in input parameters. This was clearly seen in our comparison figures, where some of the simulated trajectories differed drastically from the actual throw. The results also showed different degrees of deviation, depending on the throwing type.

We then discussed the sensitivity of the parameters and what potential errors might have affected the results. Here we also discussed our statistical findings, looking at the correlation between speed and spin, and the roll angles in relation to the landing zones.

We therefore concluded that the model could produce trajectories similar to the actual throws. However, with the model's sensitivity combined with the potential flaws of our analytically produced parameters, an accurate comparison could be difficult to achieve for all throws.

Preface

As fans of the sport disc golf, we were thrilled to get the opportunity to complete our bachelor's degree in mechanical engineering at the University of Stavanger (UiS), with a fun and challenging thesis regarding the testing and simulation of disc golf trajectories.

We would like to thank Dr. Knut Erik T. Giljarhus, our supervisor, for providing us with a great thesis, the script for the mathematical model used in our study and excellent guidance throughout this period. Next, we would like to thank the PDGA-rated athlete performing the throws for our experiment, Magnus Moseng.

We would also like to thank our professors and fellow students at UiS for contributing to three memorable years. Despite the pandemic, we have thoroughly enjoyed our time here.

Contents

List of Figures

List of Tables

Nomenclature

Acronyms	Description	units
2D	2- Dimensional space	
3D	3-Dimentional space	
DLT	Direct Linear Transformation	
MEMS	Micro-Electro-Mechanical System	
GPS	Global positioning system	
IMU	Inertial measurement data	
Pitch	Disc angle	deg
Roll	Disc angle	deg
Nose	Disc angle	deg
M	Pitching moment	Nm
p	Angular rate	rad s^{-1}
Ω	Disc spin rate (Omega)	rad s^{-1}
I	Moment of inertia	kg m^2
RHBH	Right-handed backhand	
Hyzer, Flat, Anhyzer	Different roll angles when releasing a disc	
F_D	Drag force	N
F_L	Lift force	N
q	Dynamic pressure	N m^{-2}
C_D	Drag coefficient	
C_L	Lift coefficient	
C_M	Moment coefficient	
D	Disc diameter	m
S	Disc surface	m^2
Φ, θ, ψ	Roll, pitch and yaw Euler angles	rad
T	Transformation matrix	

u, v, w	Body velocity components	m s^{-1}
β	Angle of sideslip	rad
α	Angle of attack	rad
g	Gravitational force	N
ω	Angular velocity	rad s^{-1}
F	Force vector	N
m	Mass of disc	kg
N	Number of values	
RC	Remote controlled	
FPS	Frames per second	s^{-1}
RPS	Revolutions per second	s^{-1}
RPM	Revolutions per minute	min^{-1}

1 Introduction

Disc golf is a rapidly growing sport worldwide. In the USA from 2019 to 2020, the Professional Disc Golf Association (PDGA) experienced a growth of 33% in memberships, ending the year with 71 016 members (PDGA, 2021). One of the reasons for such growth is undoubtedly the low barriers of entry. It is a simple and inexpensive sport to get into. A player only requires a disc which is usually priced around $15 a piece, and most of the courses are free of charge to play, which makes it easy for new players to try it out.

The objective and the rules of the game are in many ways similar to traditional golf, but in disc golf you use a variety of flying discs instead of golf clubs. The goal is to throw the disc, in as few attempts as possible, into a designated basket. To manage this, it´s helpful to know how the different discs will act in the air, at different angles and speeds, to find the best possible path through the course.

There are three main categories of discs. A driver, a mid-range and the putter. These discs are shaped quite differently which results in drastically different flight characteristics. Drivers can be thrown the furthest and the putters are meant for shorter flights. Coherent with its name, the mid-range is used for the throws that should be somewhere between driver- and putter range.

1.1 Thesis objective

The objective of our thesis is to experimentally test and validate a mathematical model that simulates the trajectory of a thrown golf disc.

In order to complete the objective, we had to perform a field test to gather data. The field testing was done in an open environment with multiple cameras operating. An athlete performed 30 throws with different release angles, and we recorded the results.

We then analyzed the results of our field test and produced input parameters for the simulation model. With input parameters, we could test how well the simulation could reproduce an actual throw.

1.2 Learning outcome

Through the course of our study, our knowledge on disc golf and disc trajectories increased substantially. Working on this study, it gave us an understanding of how different parameters affect the path of a disc and how to achieve the wanted trajectory with different throwing types.

In the field of experimental studies, we have gained knowledge on how to perform experiments and how to analyze data. Also, a basic understanding of aerodynamics and gyroscopic effects was obtained.

1.3 Limitations

Throughout the experimental testing process, time was a limiting factor. Aligning the logistics required for our experiment, and with most of our time used for analyzing footage, a more extensive study could have been performed, given a larger timespan. We performed a study of 10 backhand throws with three types of release angles, a total of 30 throws. Ideally, we would have performed more than 10 throws for each category to get a larger amount of data to analyze. In addition to this it would have benefited the validation of the model to test multiple types of throws. Testing a broader range of disc models would also have given more data to analyze.

Our experiment was performed with a setup which did not allow for analyzing the speed of objects in a true 3D space. The speed parameter was therefore found using trigonometric functions with a base speed found in the 2D space.

2 Literature review

In this chapter we will present some of the previous work and literature on flying discs and simulation of disc trajectories, motion capture systems and treatment of experimental data. At the end there will be a table of the search method and relevant results that were found.

While reviewing the relevant literature, we have found plenty of research done on frisbees, and less on disc golf as a sport. Kamaruddin (2011) and other studies related to our thesis, provided an understanding on the subjects of flight paths and simulations of a frisbee. What we have yet to find is a study of the flight path that extends to more than short distance throws (<20m). We have not found previous studies that included a disc golf disc, where they tested a simulation of a full range throw in a realistic environment. There are some similarities with our thesis and previous studies but the main difference from our study and the studies like Kamaruddin (2011), is that we performed our experiment in a real-life environment, achieving a full range trajectory study. This will contribute to validate the mathematical model we are testing.

2.1 Motion capture systems

For the motion capture system in Koyanagi and Ohgi (2010), the Direct Linear Transformation (DLT) method was used. This is a calibration method used to determine the pinhole camera parameters, using up to six corresponding points from 2D and 3D. In "*Design and evaluation of a new three-dimensional motion capture system based on video*" (Castro et al., 2006) the authors introduce the off-line system SOMCAM3D. For sufficient accuracy in 2D and 3D measurement, this method also uses the DLT method, with their own designed calibration device. This method offers an automatic digitalizing process, where the system automatically tracks markers attached to the object. This allows for great precision when analyzing and finding parameters related to the movement of the object.

One aspect of experiment was being able to calculate the release parameters of disc throws. Throughout the study we found several different approaches to determine the important parameters such as velocity of the disc, different angles, and spin rate. In the article Lee et al. (2017) they installed a small onboard sensor module on the disc, consisting of a three-dimensional Micro-Electro-Mechanical System (MEMS) magnetometer and accelerometer. By

using GPS and inertial measurement data (IMU), the exact position and speed of the disc during the throw could be stored on the SD card. To calculate the rotational speed, three methods were presented in this article, the use of a gyroscope, accelerometer, and magnetometer. The gyroscope is precise but has its limitations regarding angular speed over 2000 deg/s, and due to more weight added to the disc and change of the aerodynamic coefficient, the results may be affected by that. The accelerometer method uses the periodic properties of the translational acceleration and gravitational acceleration as the disc rotates. Since geomagnetism is always fixed, the results from the magnetometer become a sinusoidal wave as it rotates. This means that the sine wave period of the geomagnetism is equal to the rotation period of the flying disc. The advantage with this principle is the accuracy of measuring the rotational period regardless of the placement and angle of the device (Lee et al., 2017).

Another approach is the one used in Koyanagi and Ohgi (2010). They used a tri-axial accelerometer in combination with high-speed cameras to capture the initial start and end parameters. The accelerometer gives an estimated value for the angular velocity of the disc, which then was validated by the high-speed cameras. By placing a mark on the disc and comparing frame by frame at the release- and end point, a good estimation of the angular velocities can be made. They placed cameras in both the release and end phase, but the flight distance they measured was only 20-30 meters.

2.2 Previous work on flight simulation

Presented in Hubbard and Hummel (2000), they tested atypical, right-handed, backhand throw for 0.5s and 1s. In this experiment the disc was thrown rather slowly, with low velocity, low spin and a high angle of attack. They then concluded that further work on the subject was needed, to make the estimates of the flight coefficients from flight data more reliable and meaningful. This would mean considerably longer experimental flights and more accurate kinematic data acquisition techniques. In Hummel and Hubbard (2002), they used MATLAB to simulate a flight path, but only for a flight distance between 2 and 20 meters. Here they describe a method using an iterative algorithm to find the set of parameters, later used in their simulation. To track the disc, they used standard DLT methods for recording the xyz locations.

Finally, Hummel (2003) investigated the flight simulation of a normal frisbee. She stated that "There are no real-life conditions that will produce a perfectly horizontal straight flight, but a close approximation to this trajectory can be made. Analysis of this type of flight is useful for interpreting the relationship between angle of attack and velocity" (Hummel, 2003, p. 21). The assumptions made were rolling and pitching moment assumed to be zero, to prevent any wobble. To collect in-flight data in this article, two experiments were performed. One short flight of 2 meters, and one long flight with distance of 18 meters.

In Crowther and Potts (2007), a mathematical model was implemented in MATLAB to simulate flight trajectories of spin-stabilized sports discs. The steady model parameters were obtained by wind tunnel tests, and the unsteady parameters form flight tests. Their findings showed that the simulation was in reasonable agreement with the experimental tests, but with limited experimental flight data. They also found that a pitch angle between approximately 10° and 20° resulted in maximum length and flight time. An initial roll angle of -6° was found to create the straightest flight.

2.3 Treating experimental data

In "Statistical Treatment of Experimental Data" (Young, 1962), we learn about the different errors that may occur, and how to account for them in our study. The book covers what kind of errors one may come across, and how the propagation of errors can affect an experiment.

In "Experimentation, validation, and uncertainty analysis for engineers" (Coleman & Steele, 2018), we gathered some knowledge about the different stages in an experimental program. This book was mainly used to gather basic knowledge in the field of conducting experiments.

2.4 Search method

Table 1: Disc related search

Search word	**Name of article**	**Author(s)**	**Year of release**	**Quoted**	**Search Engine**
"Flying discs"	Dynamics and performance of flying discs	N.M Kamaruddin	2011	14	Google Scholar
"Sports disc"	Simulation of a spinstabilised sports disc	W.J Crowther, J.R Potts	2007	17	Google Scholar
"Frisbee flight"	Simulation of frisbee flight	M Hubbard, S Hummel	2000	34	Google Scholar
"Flying disc measurement"	Measurement of kinematics of a flying disc using an accelerometer	R Koyanagi, Y Ohgi	2010	5	Google Scholar

Table 2: Motion capture system

Search word	**Name of article**	**Author(s)**	**Year of release**	**Quoted**	**Search Engine**
"Motion capture system"	Design and evaluation of a new three-dimensional motion capture system based on video	J.L.G Castro, R Medina-Carnicer, A.M Galisteo	2006	67	Google Scholar

Table 3: Treating experimental data

Search word	**Name of article**	**Author(s)**	**Year of release**	**Quoted**	**Search Engine**
"Experimental data"	Statistical Treatment of Experimental Data [Book]	H.D Young	1962	949	Google Scholar
"Validation, uncertainty, engineers"	Experimentation, validation, and uncertainty analysis for engineers"	H.W Coleman, W.G Steele	2018	4637	Google Scholar

3 Theory

In this chapter, we will present the relevant theory used in the process of conducting our thesis. The chapter is divided into three parts. In the first part we will focus on disc dynamics. Here we will explain some of the theory behind flying discs, and how the discs behave during their flights. It was important for our study that we acquired a greater knowledge concerning the parameters that impact the flight of the discs. In the second part we will look at the mathematical model used to simulate the trajectories. Finally, we will present theoretical background relevant for the accuracy of our experimental procedure.

3.1 Disc dynamics

A flying disc requires two components to be able to fly properly, spin and speed. Without spin, the disc would not have any stability, and without speed the disc would not be able to create any lift. The basic principle of a flying disc is that the aerodynamic properties must create a greater lift force than the gravitational force. The disc will need what is known as the gyroscopic effect, in order to fly straight.

The gyroscopic effect comes from the pitching moment (M), which translates into a rolling motion. The disc tries to resist the pitching moment, or torque, perpendicular to the spinning axis, but ends up with a rolling motion with angular rate *p*, perpendicular to both the spinning and pitching moment axes. The mathematical formula for this gyroscopic relation can be written as,

$$M = p \times I\Omega \tag{3.1}$$

Where Ω is the disc spin rate, which is assumed to be constant, and I represents the moment of inertia of the disc (Kamaruddin, 2011).

Simply explained, the lift force is created by an unequal pressure around the disc. Firstly, by the differences in air pressure between the top and the bottom of the disc. Since the top is longer and "smoother", the air flows faster over the top than the bottom. This creates a low pressure at the

top and then a high pressure on the bottom part. The high pressure tries to move up to the low-pressure area, and therefore creates a lift force upwards. Also, the triangular shape of the rim catches the airflow in the front part as shown in figure 1, creating an upward pushing lift force to the disc. For the rear end, the airflow will catch the underside of the disc, also resulting in a lift force upwards (AFDA, (n.d.)).

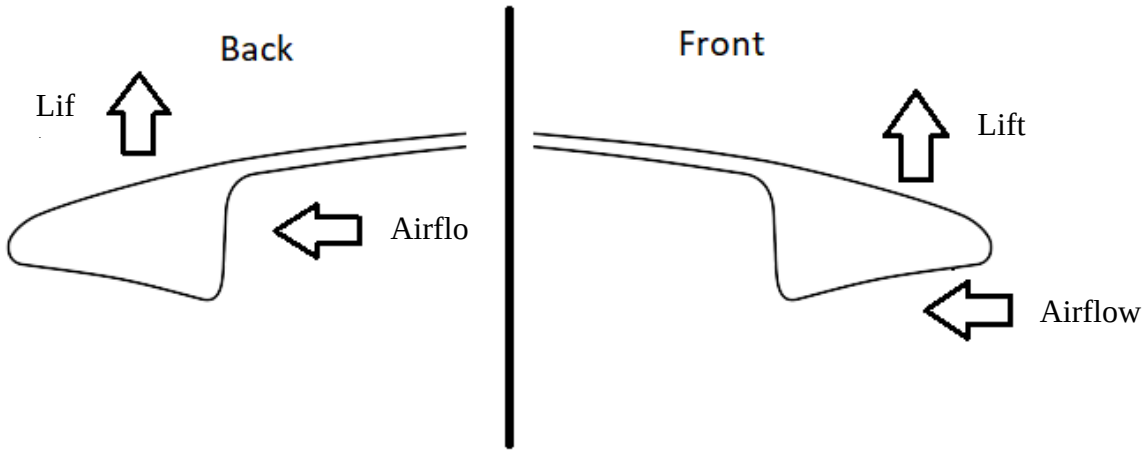

Figure 1: Lift / Airflow model

In disc golf, each disc has its own four parameters which are used as a general indicator for the flight-characteristics. These parameters are speed, ranging from 1 to 14, glide ranging from 1 to 7, turn ranging from -5 to 1 and fade ranging from 0 to 5. This rating system is created by Innova Discs, the same brand that produces the disc we are using for our experiment, and is used to compare between models, not to describe the actual flight path of the disc (Discs, (n.d.)).

In disc golf, speed is an indicator of how much power is needed to get the full potential of the throw. Speed 14 is the fastest and 1 the slowest. Speed often depends on the thickness of the rim and has a close relation to the wind speed. With tailwind, the disc will act as if it has less speed, and with headwind it will act as if it has more speed. This will change the characteristics of the flight. Glide represents the discs ability to maintain the loft. The turn stat on a disc represents the disc's ability to turn to the right at the first part of the throw, when throwing right-handed backhand throw (RHBH). +1 is more resistant to turning over and –5 turns the easiest. Turn is also known as high-speed turn because it happens at the start of the throw when the disc has the most speed. The turn is created by the gyroscopic effect that the disc experiences. Fade, also

known as low-speed fade, represents the discs tendency to cut to the left at the end of the flight, with an RHBH throw. For fade, 0 has the straightest finish and 5 will cut the most to the left (Discs, (n.d.)).

When performing throws in disc golf, one of the main deciders for what course the trajectory will take is the roll angle. When focused on RHBH throws, there are mainly three different types of releases, which will produce three drastically different paths. These are hyzer release, flat release and anhyzer release. An illustration is shown in figure 2.

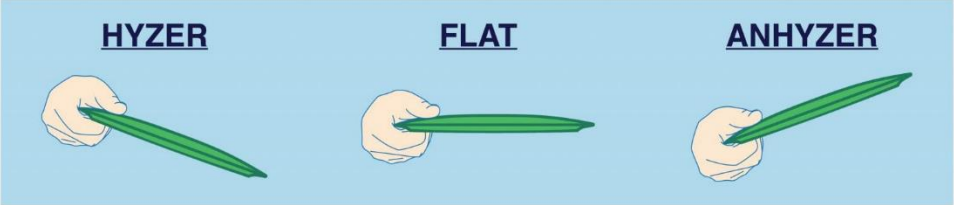

Figure 2: Different release angles (Norton, 2017)

3.2 Mathematical model

The mathematical model in use, developed by Knut Erik Teigen Giljarhus, is implemented in python to simulate the flight path of the disc. It is based on the rigid body dynamics from studies done by Hummel (2003) and Crowther and Potts (2007), later verified by Kamaruddin (2011). The model is designed to simulate trajectories utilizing the input parameters from the release point of the throw.

Through 3D-scanning and CFD simulations, forces and pressure over the disc surface is determined. These are used to calculate the aerodynamic coefficients such as moment, drag and lift through the standard definitions:

$$F_D = qC_DS \quad 3.2$$

$$F_L = qC_LS \quad 3.3$$

$$M = qC_MDS \quad 3.4$$

Where C_D, C_L and C_m represent the drag, lift and moment coefficients. The Dynamic pressure $q = 0.5\rho U^2$ and S is the disc surface (Giljarhus, 2022).

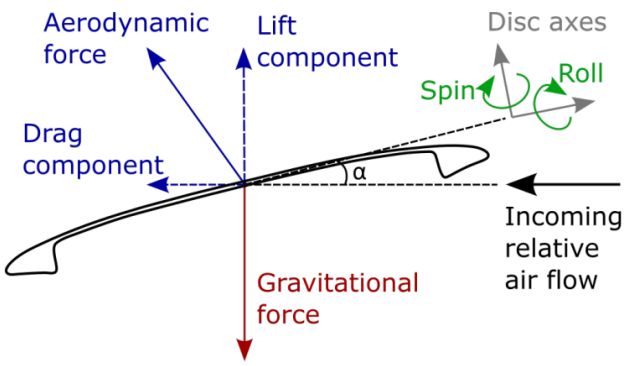

Figure 3: Forces acting on a disc (Giljarhus, 2022)

In order to derive the disc equations of motion, four coordinate systems are needed,

1. **Earth axes, $(xyz)_1$**
2. **Disc axes, $(xyz)_2$**
3. **Zero sideslip axes, $(xyz)_3$**
4. **Wind axes, $(xyz)_4$**

The only difference between the axes system used in the simulation model and the axes presented in above is that the z-axis is pointing upwards rather than downward.

Figure 4 illustrates the relationship between the earth- and the disc axes coordinate systems. It describes how the rotations from the earth axes into the body axes are achieved, using Euler roll (φ), pitch (θ) and yaw (ψ) angles (Kamaruddin, 2011).

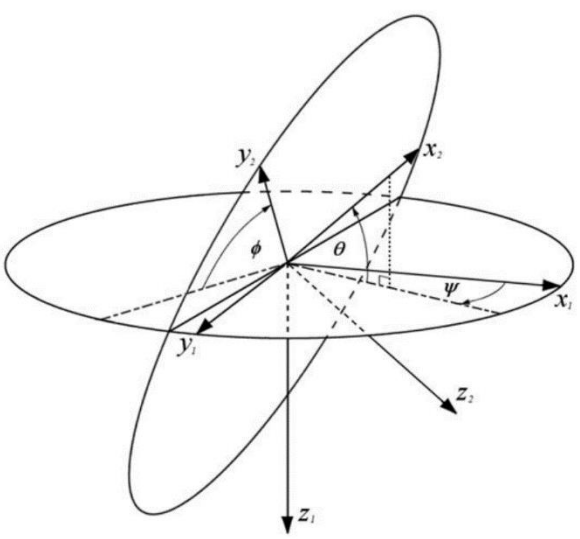

Figure 4: Relationship between Earth axes and Disc axes

Figure 5 illustrates the zero sideslip axes and the wind axes. The angle of attack of the disc is achieved through a rotation from the zero sideslip body axes into the zero sideslip wind axes. The corresponding coordinate transformations between these different axes have been detailed in Crowther and Potts (2007); (Kamaruddin, 2011).

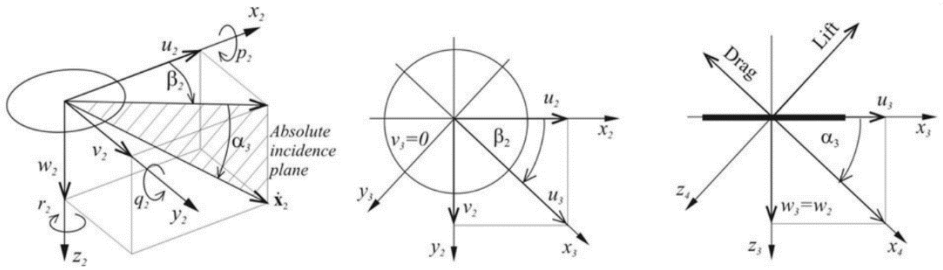

Figure 5: Zero sideslip axes, wind axis and angle of attack through rotation

To be able to transform the vector components between the different axes systems, a series of transformations are needed (Crowther & Potts, 2007). The transformation matrices presented below are used in the simulation model for the rigid body dynamics model. These have been found from Crowther and Potts (2007) and used in a slightly altered form. The only difference between the matrices in Crowther and Potts (2007) and the ones in the simulation model is the previously mentioned z-axis pointing upward instead of downwards.

$T_{12}(\theta)$ is representative for the transformation between the earth axes $(xyz)_1$ and the disc axes $(xyz)_2$, hence the numbers 1 and 2.

The following equations and descriptions are found in (Giljarhus, 2022).

$$T_{12}(\theta) = \begin{bmatrix} cos\,\theta\,cos\,\psi & sin\,\varphi\,sin\,\theta\,cos\,\psi - cos\,\varphi\,sin\,\psi & cos\,\varphi\,sin\,\theta\,cos\,\psi + sin\,\varphi\,sin\,\psi \\ cos\,\theta\,sin\,\psi & sin\,\varphi\,sin\,\theta\,sin\,\psi + cos\,\varphi\,cos\,\psi & cos\,\varphi\,sin\,\theta\,sin\,\psi - sin\,\varphi\,cos\,\psi \\ -sin\,\theta & sin\,\varphi\,cos\,\theta & cos\,\varphi\,cos\,\theta \end{bmatrix} \quad 3.5$$

$$T_{23}(\beta) = \begin{bmatrix} cos\,\beta & -sin\,\beta & 0 \\ sin\,\beta & cos\,\beta & 0 \\ 0 & 0 & 1 \end{bmatrix} \quad 3.6$$

$$T_{34}(\alpha) = \begin{bmatrix} cos\,\alpha & 0 & -sin\,\alpha \\ 0 & 1 & 0 \\ sin\,\alpha & 0 & cos\,\alpha \end{bmatrix} \quad 3.7$$

$$T_{14}(\theta)a = T_{12}(\theta)T_{23}(\beta)T_{34}(\alpha)a \quad 3.8$$

$$T_{21}(\theta) = T_{12}(\theta)^T \quad 3.9$$

From the initial condition the velocity of the disc can be converted to the disc axes using the attitude vector,

$$u_2 = T_{12}(\theta)u_1 \quad 3.10$$

Here, the wind velocity can also be included by subtracting from the initial velocity. By then using the horizontal velocity components in the disc axes, the sideslip angle is found,

$$\beta - arctan\,2\,(v_2, u_2) \quad 3.11$$

This angle is used to transform the zero sideslip axes,

$$u_3 = T_{23}(\beta)u_2 \quad 3.12$$

Using the velocities from this coordinate system the discs angle of attack can be found,

$$\alpha - arctan\,2\,(w_3, u_3) \tag{3.13}$$

In the last step, the velocity can be converted to the wind axes by rotating around this angle of attack,

$$u_4 = T_{34}(\alpha)u_3 \tag{3.14}$$

Now, together with the aerodynamic coefficients from the CFD simulation and Equations 1 and 2 the forces can be calculated by,

$$F_4 = g_4 + [-F_D, 0, F_L]^T \tag{3.15}$$

Here, the gravitational force, g_1 =[0,0,-mg]^T, is also transformed,

$$g_4 = T_{14}(\theta, \beta, \alpha)g_1 \tag{3.16}$$

Assumptions for the attitude vector are that the spin rate is constant, and the model only considers the roll of the disc caused by gyroscopic precession. This is a simplification assuming the disc is thrown without any wobbling during the release. The roll occurs in the zero sideslip axes, hence the expression for the angular velocities is,

$$\dot{\theta_3} = \left[-\frac{M}{\omega(I_{xy} - I_Z)}, 0,0\right]^T \tag{3.17}$$

Here, the moment is calculated using the coefficient of moment from the CFD calculation, Equation 3, and the moments of inertia, I_{xy} and I_z, are found from the geometry models. ω is the angular velocity of the disc. These values are finally transformed back to the ground coordinate system before advancing the simulation,

$$mu_1 = T_{41}\dot{(}\theta, \beta, \alpha)F_4 \tag{3.18}$$

$$\theta_1 = T_{31}\dot{(}\theta, \beta)\theta_3 \tag{3.19}$$

The actual integration is performed using numerical integration routines from the SciPy library (Giljarhus, 2022).

3.3 Treatment of experimental data

3.3.1 Uncertainty

Determining the uncertainties of multiple values can be executed as presented in Figure 6. Where x is a collected value, and N is the number of values collected.

Mean (x_{avg})	The average of all values of x (the "best" value of x)	$x_{\text{avg}} = \frac{x_1 + x_2 + \cdots + x_N}{N}$
Range (R)	The "spread" of the data set. This is the difference between the maximum and minimum values of x	$R = x_{\max} - x_{\min}$
Uncertainty in a measurement (Δx)	Uncertainty in a single measurement of x. You determine this uncertainty by making multiple measurements. You know from your data that x lies somewhere between $x_{\max}$ and $x_{\min}$.	$\Delta x = \frac{R}{2} = \frac{x_{\max} - x_{\min}}{2}$
Uncertainty in the Mean (Δx_{avg})	Uncertainty in the mean value of x. The actual value of x will be somewhere in a neighborhood around x_{avg}. This neighborhood of values is the uncertainty in the mean.	$\Delta x_{\text{avg}} = \frac{\Delta x}{\sqrt{N}} = \frac{R}{2\sqrt{N}}$
Measured Value (x_m)	The final reported value of a measurement of x contains both the average value and the uncertainty in the mean.	$x_{\text{m}} = x_{\text{avg}} \pm \Delta x_{\text{avg}}$

Figure 6: Calculating uncertainty (Astronomy, (n.d.))

3.3.2 Errors

When performing experiments, there will often be errors occurring. Deciphering between systematic errors and random errors is therefore important.

Systematic errors are errors associated with the particular instruments or technique of measurement being used (Young, 1962).

Random errors are on the other hand errors produced by a large number of unpredictable and unknown variations in the experiential situation. They can result from small errors in judgment on the part of the observer, such as estimating tenths of the smallest scale division (Young, 1962).

3.3.3 Correlation

Correlation is a measurement of the relationship between two variables. The correlation differs between -1< 0 < 1. A correlation of exactly 1 means that there is a 100% positive correlation between the two variables, meaning that they will increase at the same rate as the other, and opposite for a value of -1. A perfect correlation will result in a perfect straight line in the plot pointing to the right or left from origin depending on the value. The more the value approaches zero, the less the correlation (Bewick et al., 2003; Tjelmeland, 2017).

4 Method

In this chapter we will introduce our test plan and the elements included in each stage. Secondly, we will elaborate in further detail the topics of experimental setup and analysis.

The test plan consists of five main points, carried out in the same order as presented below:

1. **Gathering of information**
    a. Previous studies
2. **Interactions with our supervisor** *(Consecutively throughout the study)*
    a. Open line of communication
    b. Meetings
3. **Pre-experimental Stage**
    a. Trial-and-error phase (*Setup*)
    b. Trial-and-error phase (*Analytical Testing*)
4. **Performing the experiment**
    a. Recording results
5. **Post-experimental Stage**
    a. Analytic Results
    b. Statistical Results
    c. Presentation of Results

At first, we performed a search of literature, increasing our knowledge in the field of Aerodynamics and experimental testing. We found similar thesis statements, and relevant articles that described simulations of trajectories performed with discs. This was to ensure a certain understanding of the context the experiment we were conducting was in.

Meetings were held frequently with our supervisor, ensuring that the process was moving forward with common understanding. In these meetings we also collected valuable information concerning our analysis process and the analytic tools utilized in our experiment. Thoughts and ideas on how to perform the experiment to the best of our ability was also an often-discussed topic.

Our first trial-and-error stage was related to the practicalities of the experiment. This stage consisted of testing out different placement combinations of our motion-capture system. The second stage was to test out the analytical side of the experiment. Performing multiple trials containing tests of tracking ability and how well we could collect the necessary angle information. It was also in this stage that we first started placing out markers to be able to calibrate our systems. These trials proved valuable for the purpose of optimizing the experimental setup, which we will explain in the next sub-chapter.

4.1 Experimental Setup

4.1.1 Preparations

In order to perform an experiment that consists mainly of post-experimental analysis, the importance of being well prepared is crucial. The experiment had certain testing criteria that needed to be met for us to begin producing a testing plan. The first criteria was finding the large space needed to perform the throws. Considering the disc we were testing, flight distances over 100 meters could be reached with ease. Therefore, we had to ensure that the field was sufficient for performing these kind of throws.

During the last few years, we have used a local football field to test our new discs and try out certain throws. Therefore, it was rather obvious to us that it would be a good location for the experiment at hand. We conducted five separate test-runs, each consisting of multiple throws and a large gathering of information. This information essentially gave us the knowledge to create our final setup. Small adjustments of the camera angles and the drones hovering height would ensure that we had a sufficient setup for the experiment.

Before this, we had to make sure that we could fly a drone in the area considering the strict rules and regulations for flying drones and similar RC aircraft. For drones weighing less than 250 grams, with an onboard camera, the rules state that you can fly up to 120 meters above ground, without a need for a license. The only step needed is registering the drone online before flying. We used the DJI Mini 2, which weighs 249 grams, so there were no issues with legal regulations for our experiment.

4.1.2 Motion capture systems

4.1.2.1 Ground cameras

We used three GoPro hero 10 black cameras stationed on the ground to capture the initial part of the throw. These cameras provide videos in 2704 x 1520 resolution and a frame rate of 240 FPS. The high resolution and framerate make it possible to measure angles with high precision for each frame. One camera was placed behind the athlete (back view), and one capturing the throw from the side (sideview), both placed on a tripod at throwing height. The third camera was placed on the ground in front of the release area filming with an angle upwards (ground view).

The purpose of the side view camera was to determine the nose- and pitch angle. The back view camera captured the roll angle, and the camera on the ground captured the rotational speed of the disc. With 240 FPS we were able to determine the rotational speed by inspecting one frame at the time. Using the black and white line on the disc as reference, we could see how many frames it took for the disc to make a full rotation of 360 degrees, see Figure 7.

Figure 7: Disc with spin-tracking line

4.1.2.2 Drone

In order to get a video of the disc's full trajectory, we had to have a camera at an altitude of about 95 meters above ground. A drone was used for this purpose. The height was found by testing out different hoovering heights to see if it could capture the full flight path. The drone for the mission was the DJI Mini 2. This drone weighs 249 grams and takes in use of a 3-axis stabilizer providing us with a resolution of 3840 x 2160 at 30 frames per second.

The drone is placed approximately 40 meters away from the point where the disc is released. It could then produce a video that covered the entire path of the disc.

4.1.2.3 Calibrations

To be able to analyze the footage, we needed to calibrate the motion capture system. For the drone view camera, we measured up 50 meters of the field, and placed an object that we were able to use for calibrating distances in Tracker. Calibrating the drone view was essential, as we used this footage to calculate the discs speed and distance traveled.

Our side view and back view also needed to be calibrated, but this time for the main axis system used in Tracker. For the sideview we placed out a level that was adjusted to be perfectly horizontal. The camera located behind the person throwing (back view), had a multitude of different calibration methods already available, so there was no need for preparatory work other than ensuring it was correct. The ground view camera, facing the sky, did not need calibration.

4.2 Discs

In our experiments we used five identical discs. The disc used was the Innova Wraith. The specifications for each of the discs are identical. Even though the discs are meant to be identical there were some differences that we noticed. The discs are created in plastic through the process of injection molding (Latitude-64, 2020), and because of possible differences in the production conditions, small variations in the discs can occur. It can be small material differences or the temperature and humidity under the production phase. We could feel that some of the discs were slightly more flexible and others firmer. We also noticed a slight difference in some of the discs when it came to their shape. Some had a deeper pit on the top part than others. These are small, barely visible differences, but could make a significant impact on the aerodynamics of the discs.

4.3 Analysis

4.3.1 Tracker software

For our analytic software, we are using Tracker. Tracker is a free analysis program developed on the Open-Source Physics Java framework. Originally developed for use in physics education (Douglas Brown, 2022), it provides a variety of useful tools for challenges like ours. It allows us to track a moving object and after calibration give outputs like velocity, distance and position frame by frame, as well as determining angles of the moving object. We used the software on all the videos from the four different cameras.

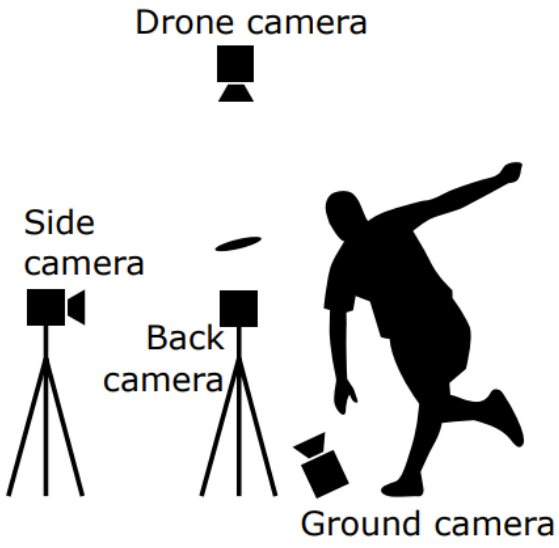

Figure 8: Camera setup (Giljarhus, 2022)

4.3.2 Drone video

When analyzing the drone footage, we identify the disc, and mark its center from the release point. After marking the object, the program has a “auto-track” function that follows the flight and automatically searches the next frame for an object of the same size and color. Small track points are created as it walks through every frame of the video. The process looks like this.

Figure 9: Drone footage tracking

If the software makes an error at some stage and places a point where it's not supposed to be, you can easily move it to the correct position. It is therefore important to follow the software frame by frame to ensure that it is as correct as possible.

When the software has provided us with all the track points needed, we can view the path (Figure 10). We also calibrate the image in relation to the 50-meter mark we had put out. Tracker will then register the calibrated length and be able to calculate the velocity of the disc at each given point from the tracking process, as well as the distance in x-direction and y-direction. The results were presented in a table and as a dataset with x- and y coordinates at each frame, see Figure 11.

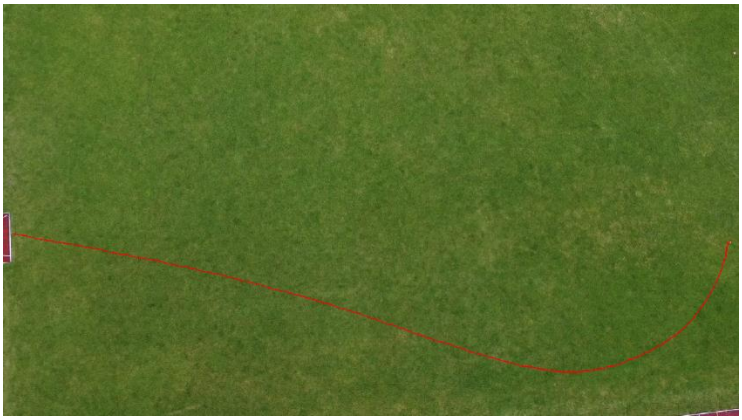

Figure 10: Drone footage path

Columns | mass A

t (s)	x (m)	y (m)	v (m/s)
5,900	91,14	16,49	9,004
5,933	91,41	16,64	9,565
5,967	91,71	16,78	8,164
6,000	91,90	16,88	8,101
6,033	92,17	17,08	8,336
6,067	92,36	17,19	7,307
6,100	92,58	17,34	8,552
6,133	92,84	17,50	8,144
6,167	93,05	17,61	6,438
6,200	93,23	17,68	6,527
6,233	93,41	17,85	7,043
6,267	93,61	17,94	6,917
6,300	93,80	18,10	7,177
6,333	94,00	18,23	6,465
6,367	94,16	18,33	6,236
6,400	94,36	18,44	6,419
6,433	94,52	18,57	5,680
6,467	94,65	18,68	5,505
6,500	94,80	18,80	5,751
6,533	94,97	18,90	5,687
6,567	95,12	19,01	5,276
6,600	95,23	19,13	4,374
6,633	95,33	19,21	4,846
6,667	95,49	19,32	5,402
6,700	95,61	19,43	4,728
6,733	95,72	19,53	4,374
6,767	95,83	19,63	3,140
6,800	95,88	19,67	

Figure 11: Tracking table for coordinates and speeds

4.3.3 Sideview

For our sideview footage, the first step was to calibrate the coordinate-axis. We used the level placed on the ground as reference and lined the axis parallel to it. By walking through the footage frame by frame, we find the exact point of release of the disc. Then we used the “tape measure” option in Tracker, and lined it up with the disc. The difference between the coordinate axis and the tape measure gave us the pitch angle.

Figure 12: Pitch angle analysis

The next step was to determine the nose angle. Here we used the “manual tracker”-option to track the center of the disc for the first 5-8 frames. This gave us the path of the disc as shown in Figure 13. Again, we line up the tape measure with the disc, and the coordinate axis along the path of the disc. The difference results in the nose angle.

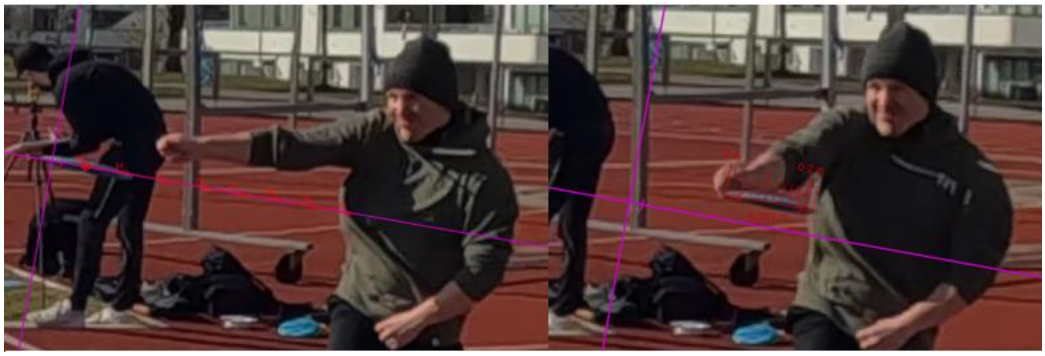

Figure 13: Nose angle analysis

4.3.4 Back view

After calibrating the coordinate axis, we find the point of release. Again, using the “tape measure” we line it up with the disc, which will then give us the roll angle in correlation to the axis.

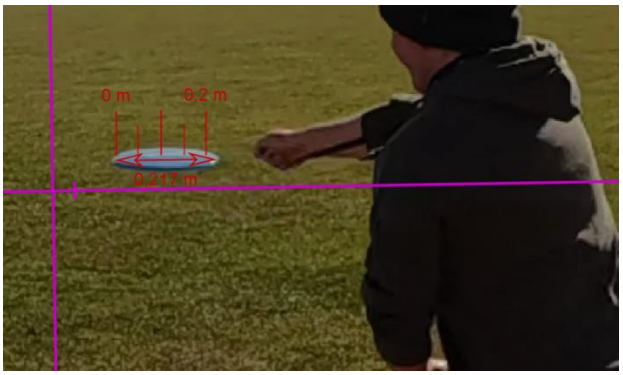

Figure 14: Roll angle analysis

4.3.5 Ground view

From the camera on the ground, we need a clear shot of the underside of the disc, where the black and white line is located. By going to the frame of release, we set the coordinate axis in line with the marked-out line on the disc. Then we count the number of frames it takes for the disc to make a full rotation, when it is lined up with the coordinate axis again. Our omega parameter is then calculated by using the number of frames per revolution, following this set of equations,

$$Time\ per\ rotation = \frac{frames\ per\ rotation}{Camera\ FPS} \quad 4.1$$

$$RPS = \frac{1}{Time\ per\ rotation} \quad 4.2$$

$$RPM = RPS \cdot 60 \quad 4.3$$

$$Omega = 2\pi \cdot RPS \quad 4.4$$

Where frames per revolution is the measured value and Camera FPS = 239,76

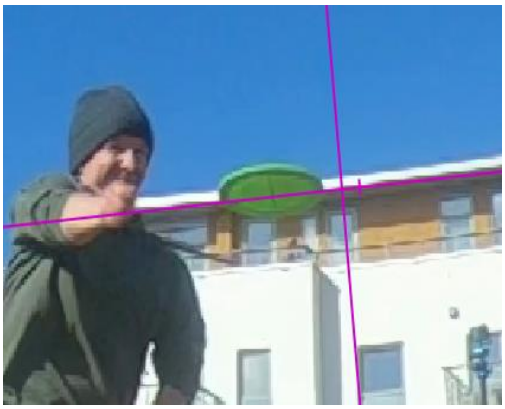

Figure 15: Spin analysis

4.3.6 Wind

In our experiments we used the Kestrel 5500 Weather/Environmental Meter to measure the wind speed. The device is placed on top of a tripod and attached to a “wing” that moves freely around 360 degrees, according to the wind direction. This allows us to measure both the speed and direction. We had one placed in the throwing area, next to the cameras. By continuously taking notes of the speed through the flight we got a good estimate of the wind speed affecting the disc.

5 Results

In this chapter, we will present the results of our experiment.

In order to visualize the results from the experiment, we created plots representing the trajectories of each throw. The first subchapter, Experimental results, will be presented with a further three subchapters, each representing a different throwing form. In these subchapters you will find a combination of figures and tables, where the figures consist of the ten trajectories from the throws done in the experiment, and one simulated trajectory. The tables will present the parameters related to each throw.

Secondly, in the next subchapter, we will present figures that compare the results from a variety of different throws to the simulated trajectory created by the model. These figures will show how well the simulation compares to an actual throw.

The third subchapter we will present the uncertainties that we have found in relation to each parameter extruded from the experiment.

Finally, we will present our statistical findings. Here we will show the correlation between speed and spin, as well as the relationship between distance and roll angle.

5.1 Experimental Results

The results of the 30 throws are presented in Table 4-6 and projected in Figure 16-18. For each category the ten throws were compared to one simulation. This is to inspect how well the mathematical model can simulate real life throws with full trajectories.

The reasoning behind the two “missing” trajectories in Figure 16 is based off the impracticalities with presenting throws that went out of range of our drone footage. They can be viewed in Appendix A, where alle throws will be presented separately.

5.1.1 Hyzer

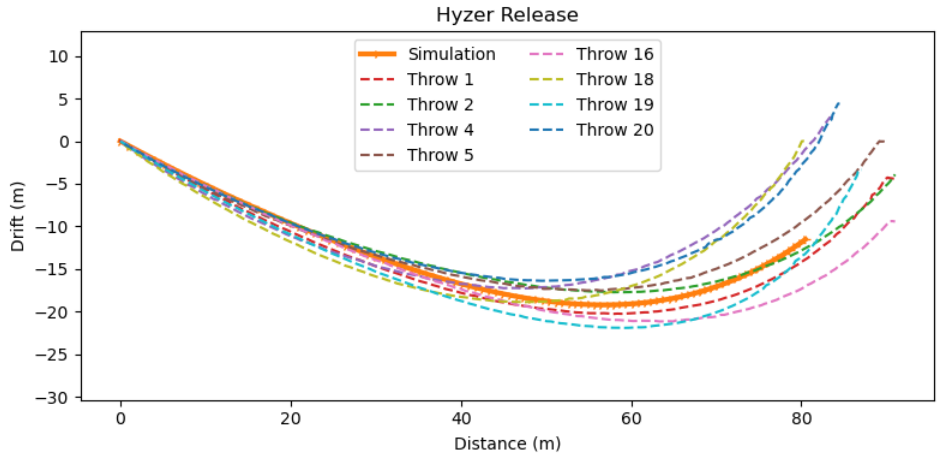

Figure 16: Hyzer release

Table 4: Parameters for hyzer throws

Throw	Pitch (°)	Roll (°)	Nose (°)	Speed (ms^{-1})	Omega ($rads^{-1}$)	Yaw (°)	Wind (ms^{-1})	Length (m)
1	15,5	21,8	0,0	23,4	125,5	-31,6	4,2	89,7
2	12,4	21,2	0,5	24,4	120,5	-28,3	4,2	91,5
3	16,1	19,0	-3,2	22,3	104,6	-46,1	3,8	77,0
4	19,6	27,2	3,2	23,2	113,3	-34,1	3,3	83,3
5	19,2	23	2,6	22,4	114,1	-30,0	3,6	89,3
16	12,5	21,6	0,0	24,5	125,5	-29,0	1,0	90,0
17	11,4	23,2	2,1	24,5	117,7	-36,3	1,3	97,8
18	19,9	25,7	0,0	23,1	115,0	-35,2	1,1	81,0
19	20,6	22,7	0,0	23,4	114,1	-32,2	1,1	87,0
20	23,3	21,9	1,8	23,8	115,0	-29,5	0,9	85,0
Sim	14,0	22,0	0,0	24,5	135,0	-28,5	4,2	80,6

5.1.2 Flat

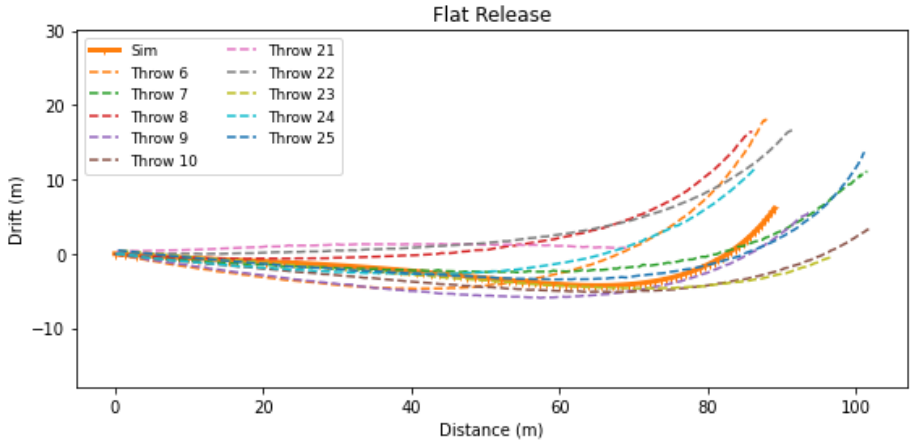

Figure 17: Flat release

Table 5 Parameters for flat throws

Throw	Pitch (°)	Roll (°)	Nose (°)	Speed (ms^{-1})	Omega ($rads^{-1}$)	Yaw (°)	Wind (ms^{-1})	Length (m)
6	12,3	14,7	0,8	22,7	116,8	-9,6	1,2	87,0
7	7,9	16,1	2,0	24,3	118,6	-5,9	0,9	98,2
8	11,7	16,8	0,4	23,7	111,6	-3,5	2,3	85,5
9	8,3	12,7	0,9	24,0	114,1	-9,7	1,6	92,5
10	7,2	15,7	2,6	24,8	125,5	-7,4	1,0	102,2
21	7,5	12,0	6,5	25,1	117,7	0,0	2,1	71,3
22	9,4	14,2	3,0	24,4	118,6	-3,5	1,8	91,1
23	8,0	11,6	1,5	24,8	112,4	-5,5	0,0	96,1
24	8,6	9,2	1,6	24,6	109,2	-6,0	1,1	86,7
25	9,8	12,0	1,1	24,4	114,1	-6,2	0,4	100,1
Sim	10,0	13,0	1,0	24,3	130,0	-4,0	2,0	89,3

5.1.3 Anhyzer

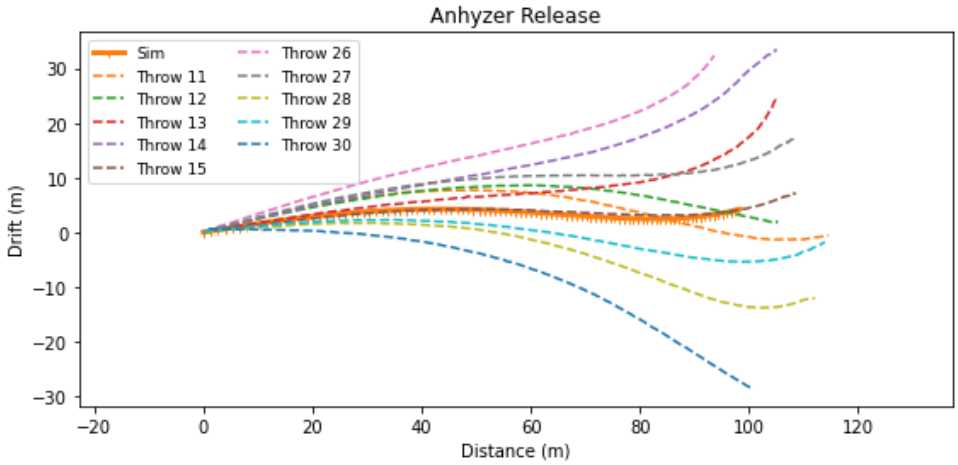

Figure 18: Anhyzer release

Table 6: Parameters for anhyzer throws

Throw	Pitch (°)	Roll (°)	Nose (°)	Speed (ms^{-1})	Omega ($rads^{-1}$)	Yaw (°)	Wind (ms^{-1})	Length (m)
11	6,0	-0,8	3.1	23,5	120,5	14,0	1,5	114,5+
12	5,3	2,0	2,2	25,2	127,7	13,4	1,7	104,8
13	10,3	-0,2	0,7	23,9	131,0	9,9	3,7	104,6
14	5,9	4,7	1.5	25,3	128,8	14,2	1,6	101,2
15	5,2	-0,7	1,7	24,6	147,7	8,0	0,8	106,6
26	6,6	0,0	1,1	24,2	134,2	20,6	1,8	93,6
27	8,0	1,2	1,7	23,6	127,7	15,1	3,5	105,8
28	7,3	-1,8	0,2	24,0	125,5	8,0	1,3	109,7
29	7,2	1,4	1,2	23,9	132,1	7,5	2,0	107,3
30	5,5	2,7	1,6	23,3	123,5	1,1	2,2	90,0
Sim	6,0	4,8	2,0	24,8	120	8,0	3.2	98,7

5.2 Comparison

In order to better portray the accuracy of the simulations, we compared all the recorded throws one by one and will now present the most- and least accurate from each category. The main reason for performing these comparisons is to see that the simulation can produce a trajectory similar to what our recorded throws show.

The green path indicates an accurate match, and on the contrary an inaccurate match with the red path. The parameters for the relevant throws are shown below each figure, with the absolute value of the differences between each parameter listed at the bottom.

Hyzer

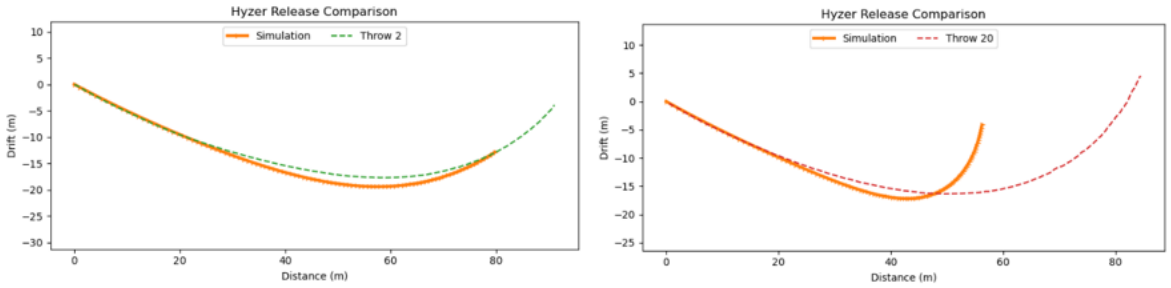

Figure 19: Hyzer comparison

Table 7: Parameters for throw 2 and 20, and the absolute value of the differences.

Throw	Pitch (°)	Roll (°)	Nose (°)	Speed (ms^{-1})	Omega ($rads^{-1}$)	Yaw (°)	Wind (ms^{-1})	Length (m)
2	12,4	21,2	0,5	24,4	120,5	-28,3	4,2	91,5
20	23,3	21,9	1,8	23,8	115,0	-29,5	0,9	85,0
Diff	10,9	0,7	1,3	0,6	5,5	1,2	3,3	6,5

Flat

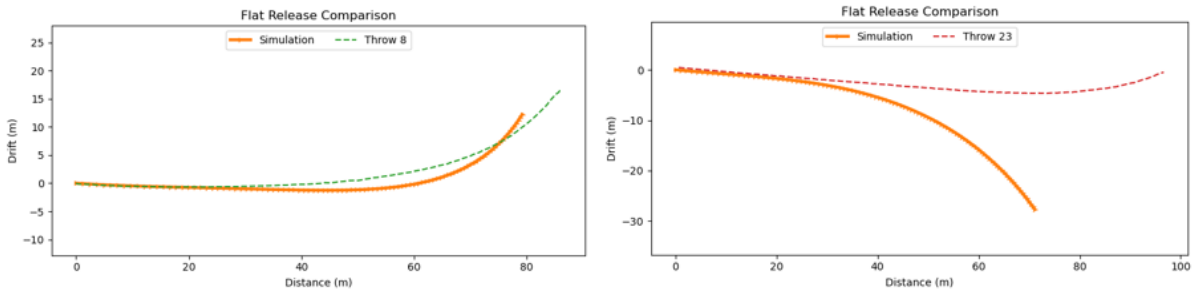

Figure 20: Flat comparison

Table 8: Parameters for throw 8 and 23, and the absolute value of the differences.

Throw	Pitch (°)	Roll (°)	Nose (°)	Speed (ms^{-1})	Omega ($rads^{-1}$)	Yaw (°)	Wind (ms^{-1})	Length (m)
8	11,7	16,8	0,4	23,7	111,6	-3,5	2,3	85,5
23	8,0	11,6	1,5	24,8	112,4	-5,5	0,0	96,1
Diff	3,7	5,2	1,1	1,1	0,8	2,0	2,3	10,6

Anhyzer

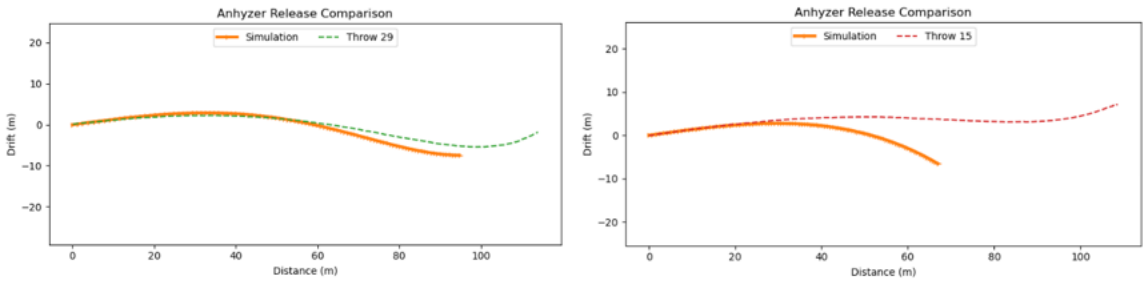

Figure 21: Anhyzer comparison

Table 9: Parameters for throw 29 and 15, and the absolute value of the differences.

Throw	Pitch (°)	Roll (°)	Nose (°)	Speed (ms^{-1})	Omega ($rads^{-1}$)	Yaw (°)	Wind (ms^{-1})	Length (m)
29	7,2	1,4	1,2	23,9	132,1	7,5	2,0	107,3
15	5,2	-0,7	1,7	24,6	147,7	8,0	0,8	106,6
Diff	2,0	0,7	0,5	0,7	15,6	0,5	1,2	1,3

5.3 Calculated uncertainties

The uncertainties related to each parameter was found by analyzing our experimental footage and using the formulas presented in Figure 6 from the Theory chapter. The uncertainties are presented in Table 10 below.

Table 10: Uncertainties of our measured parameters

Parameters	Pitch	Roll	Nose	Disc Speed	Omega	Yaw	Wind direction	Wind speed
Uncertainties	±2°	±5°	±2°	±0.6ms^{-1}	±5 $rads^{-1}$	±2°	±2°	±1ms^{-1}

5.4 Statistical analysis

To see if there was some correlation between speed and spin, we plotted speed on the x-axis and spin on the y-axis. The results from all 30 throws are presented in Figure 22. The trend-line is drawn through the points to confirm a positive correlation value, indicating that an increase in one variable will result in an increase in the other.

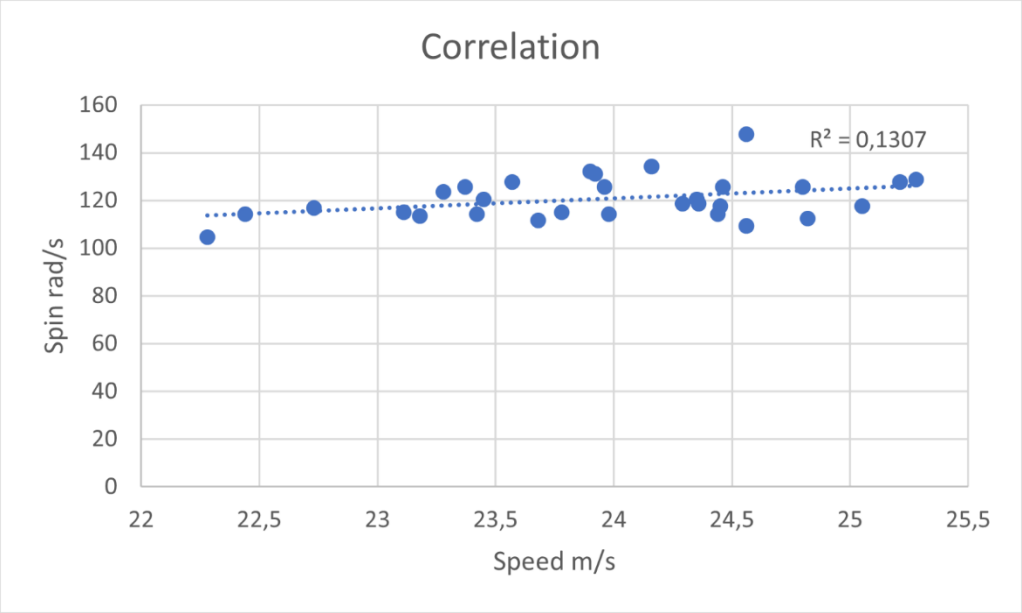

Figure 22: Correlation between speed and spin

In Figure 23, we present the roll angle and the landing zone for each throwing type, where a large spread in roll angle, will result in a large spread in landing zones.

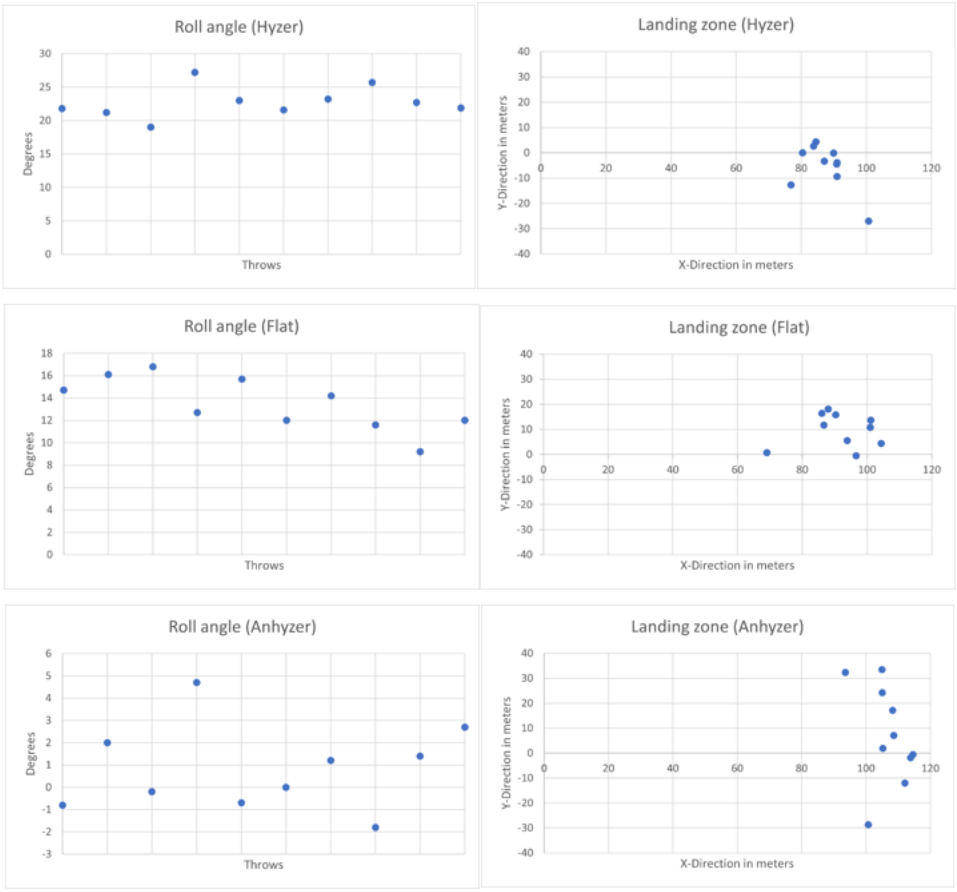

Figure 23: Roll angle and landing zones

6 Discussion

In the process of collecting and producing the results for our experiment, there were certain topics we would like to discuss. First, we will look at all the bundles of trajectories presented in correlation with the throwing type separately. Then we will discuss the sensitivity, uncertainties and the deviations that would affect the results presented.

For all three categories the simulation matches the characteristics of the flights quite well, even though the landing zones vary. The simulations prove to have a shorter flight path for all types of throws, compared to the actual throws.

6.1 Hyzer release

The high roll angle for the hyzer throws makes the discs track towards the left for the majority of the flight, with a sharper turn at the end. Presented in Figure 16, we see eight trajectories thrown with a hyzer release. They all have the same recognizable flight, with a relatively small, concentrated landing zone around the 80 m mark.

The hyzer throw was the category that provided the most compact landing zone. From Table 4 in Results, we saw that even though the roll angle varied between 19 degrees and 27,2 degrees, all trajectories had the same type of path. This might show us that the model is not that sensitive to the roll angle alone, when performing hyzer throw.

Normally, the speed and wind are also very important to determine the trajectory. Both the speed and wind contribute to determining what degree the disc will turn over and where it lands. Again, the hyzer angle eliminates the possibility of turning over, so therefore the model is not that sensitive to speed and wind when creating the trajectory. The speed and wind will be rather more important in relation to the length and how steep the leftward tracking arc is.

6.2 Flat release

The next bundle is a complete set of ten trajectories. In Table 5 we can see that the flat release has a lower roll angle. The characteristic for these flights is that the discs tend to track towards the right in the first part, before finishing with a left turn, creating a slight s-curve. Figure 17 shows a slightly larger spread in the trajectorial path and a vaguely larger landing zone, with one deviation.

Again, the simulation proves capable of producing a sufficient trajectory, but in similarity with the hyzer simulation, a tad short. The reason behind the larger spread in landing zones could come from the fact that the disc is a stable disc. The trajectory will therefore depend more on the angle of release than other discs that turn more. If it is released with a smaller roll angle, it will easily turn to the right before fading left. If the roll angle increases in the positive direction, it will, similarly to the hyzer, not turn over to the right before fading left.

6.3 Anhyzer release

The final bundle presents the ten trajectories thrown with an anhyzer release. The lower roll angle on these throws results in a slightly sharper S-curve than for flat release. The deviation of the collection is much larger on anhyzer than for the two other categories, even though most throws have similar flight characteristics.

The anhyzer depends more on a steep release angle turning it to the right at the start, but too steep, it will not be able to turn back over. The balance between a good release and a failed release is more sensitive here, similar to the flat throw. Therefore, we would expect it to be harder to produce accurate simulation for these trajectories. The reasoning behind that is that the angles we have found may differ slightly from the actual angles. Resulting in a simulation where the disc might take a completely different path based on the sensitivity of the input parameters.

6.4 Statistical findings

The correlation of the two variables, speed and spin, is simply provided to illustrate the relationship between increasing and decreasing values. We can see that there is a degree of positive correlation between speed and spin, and the correlation value r = 0,362 also reflect this. A perfect correlation will have value r = 1. This tells us that there is a relationship between an increase or decrease in speed or spin, but not a perfectly clear one. In our experiments this means that throws with higher speed will be expected to have a higher spin, although there will potentially be some exceptions from the rule.

We also investigated if there were any relations between the differences in the roll angle and the landing zones for each category, as shown in Figure 23. For the hyzer release, there were small differences in the roll angle for the majority of the throws, which resulted in a small, concentrated landing zone. For the flat release there were slightly larger deviations, and therefore slightly more spread in landing zones. The anhyzer release had large deviations in roll angle which again was reflected in the plot for landing zones.

These results agree with the results discussed above for each category.

6.5 Sensitivity, uncertainties and deviations

The precision of our results will naturally be dependent on the accuracy of our measurements. We will now discuss the parameters and their sensitivity, the uncertainties and the possible reasoning behind the deviations.

The uncertainty of the speed is found by tracking the first 5 frames after initial release. We did this repeatedly on the same throw and found an average speed, later putting the values into the formulas from the theory to establish the uncertainty. A similar process was done to get the uncertainties for the angles. Extruding values for the angle-parameters are shown in the Method chapter.

Through the process of comparing each of the actual throws with the model we found both accurate and inaccurate matches, as Figure 19-21 in Results presents. When we looked further into what could make such a big difference, we found out that the model was very sensitive to changes in the wind speed, nose angle and the speed of the disc. The wind- and disc speeds are

closely related, where an increase in tailwind would result in the disc experiencing a lower velocity. And on the other hand, if there is headwind, the disc would “feel” like it has more speed. The reason for this is that the disc will misconceive the speed it has, with the speed it experiences when actively being subjected to wind.

We knew that the wind parameter we used was just an approximate value, because we only measured the wind at the first phase of the flight. The wind will change during the different stages of the flight, depending on the altitude of the disc. The direction of the measured wind speed was also an approximate value, based on the direction the Weather Meter faced at the release area. Both these factors will affect the simulation.

A small increase in the tailwind speed will usually add some length to the trajectory, but after a certain point it will make the disc start fading at an earlier stage. This agrees with the wind- and speed relation described above. A decrease in tailwind will, on the other hand, result in more high-speed turn, especially for the flat and anhyzer throws. If the disc turns too much, the disc will not be able to fade back, and will in almost all cases result in a shorter trajectory.

The mathematical model assumes that the disc has no wobble throughout the flight. Though, in reality, this will not be the case, as we clearly could see when analyzing the video footage in slow motion. The oscillation in the disc angles create a wobbling sensation, which makes it more difficult to find the exact angles to use, because the angles differ so much from frame to frame. Therefore, through the analysis we had to look at the first number of frames of the disc to try to find the part where the wobble would least affect the disc. Figure 24 shows footage from the back view camera, illustrating the wobble as you walk through the first six frames.

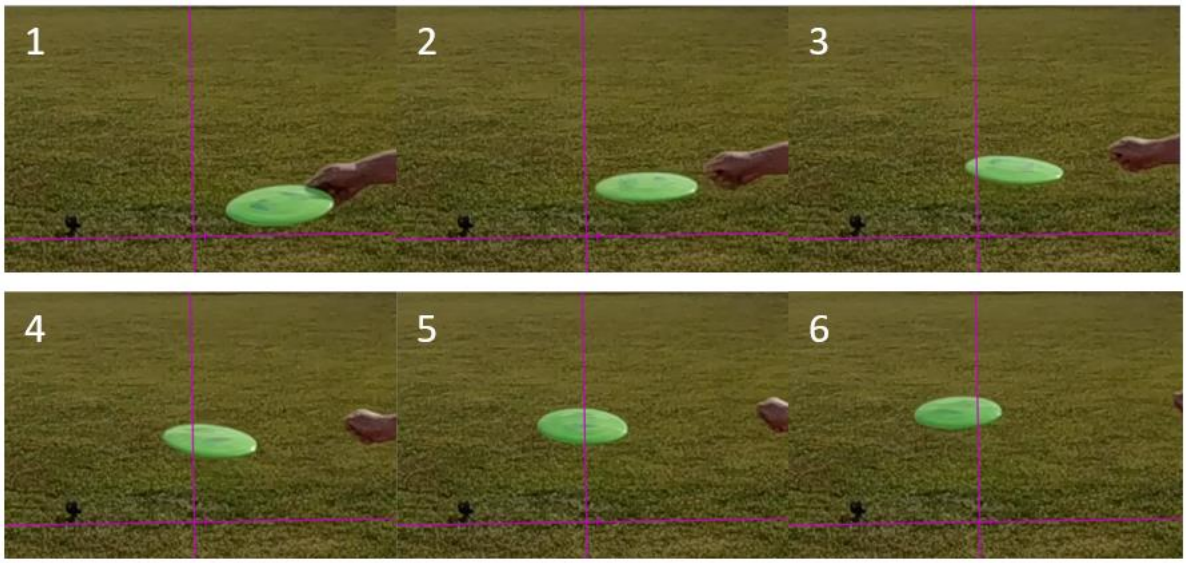

Figure 24: Wobble illustration

A parameter worth discussing is the speed of the disc. This was one of the more interesting parameters as there were large deviations in the trajectories after only a small adjustment in the speed-value. It was also a difficult parameter to determine with full precision because we calculated the speed using the footage from the drone. When filming the disc from above, it shows the speed in a 2D space. In real life the speed component will have a velocity in 3D space. Our results are based on the speed calculated in Tracker. We then use the pitch angle to compute trigonometric calculations to compensate for the speed caused by a change in altitude. This resulted in a slightly higher and more realistic speed. It is still not technically the actual speed, but considering the movement of the disc, it should produce a representative value.

6.6 Credibility of our method

In order to evaluate our method, we must discuss the flaws that have presented themselves during the timespan of this study.

6.6.1 Preparational errors

It was clear to us when we first started preparing for the experiment that there would be factors interfering with the quality of our results. Our trial-and-error phase was in many ways sufficient, but the analysis testing could have been a more comprehensive test.

The main issue with our setup was the camera angulations. Sufficient for the results we needed but not ideal for a more extensive and accurate test. Placing cameras can often be difficult, especially if there's going to be a person in between the camera and the object you want to study. In our case we had to move our back view camera to create a field of view that could allow us to study the disc as it was released from the athlete's hand. The placement of the camera provided us with a clear shot of the disc but consequently gave us a slightly angled view. Therefore, the roll angle, which was what we were looking for with our back view camera, came out slightly twisted with respect to the global axes.

7 Conclusion

To conclude this study, we would like to revisit the method used in our experiment and the main results from our analysis.

As this is the first study of a full trajectory disc golf throw, the method used is essential. We created a method that has a clear test plan, which is presented in the first part of chapter 4. Following we explain the experimental setup of our experiment, providing information concerning the camera setups and drone placement. We then proceed to show the steps of our analysis, including all steps needed to find the parameters for the simulation model. The method proved to be sufficient for our study, but it is by no means flawless.

As for the results, our main goal was to validate that the simulation model could provide a trajectory that represents, to a certain accuracy, the trajectory of a real-life throw.

As presented in chapter 5, in Figure 16-18, also presented below, the simulation can easily produce a trajectory that would be representative for the throwing type. To view all results, you may refer to chapter 5.

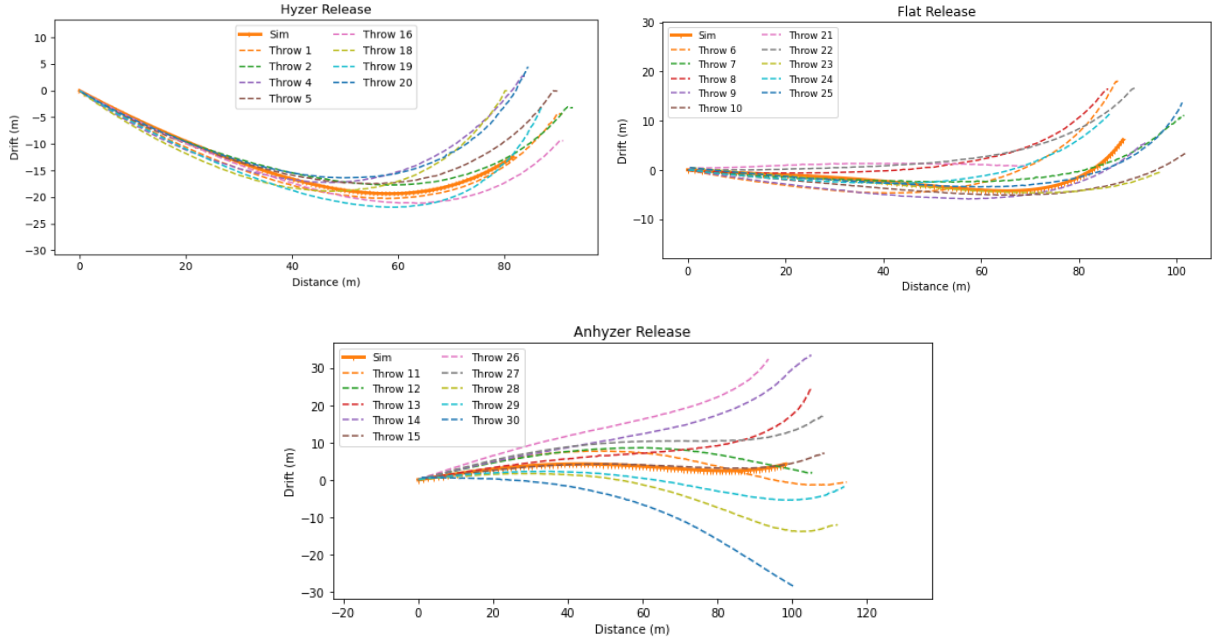

When comparing each throw to the simulation using the parameters from the real-life throw as input for the simulation model, the results were mixed. See Figure 19-21 in chapter 5. The main reason for this is, with great probability, that the sensitivity of parameters can drastically change

the path of the disc. Even a small adjustment can alternate the trajectory massively. Therefore, the accuracy of the comparisons does not purely depend on the simulation results, but simultaneously dependent on the precision of our input parameters.

7.1 Future work

For future work on the subject, there are some alterations that would be recommended. Firstly, a different camera setup could be necessary if one wanted more accurate results. Our camera placement made it difficult to find the exact speed of the disc, only a close estimate. We also encountered some difficulties when finding the accurate angles for roll, pitch and nose. Though this was consequently an error caused by wobble, and slightly suboptimal camera angulations compromising a direct and leveled field of view for studying angles. Ideally, we would also have the time and resources to perform a study of a larger number of trajectories, where we analyze different discs, and a further variety of different throwing techniques.

8 References

AFDA. ((n.d.), (n.d.)). *The Physics of Disc Flight*. Australian Flying Disc Association Limited. https://afda.com/the-physics-of-disc-flight

Astronomy, D. o. P. ((n.d.)). *Managing Errors and Uncertainty* [Calculating uncertainty]. University of Pennsylvania. https://www.physics.upenn.edu/sites/default/files/Managing%20Errors%20and%20Uncertainty.pdf

Bewick, V., Cheek, L., & Ball, J. (2003). Statistics review 7: Correlation and regression. *Critical care*, *7*(6), 1-9. https://link.springer.com/article/10.1186/cc2401

Castro, J. G., Medina-Carnicer, R., & Galisteo, A. M. (2006). Design and evaluation of a new three-dimensional motion capture system based on video. *Gait & posture*, *24*(1), 126-129. https://reader.elsevier.com/reader/sd/pii/S0966636205001372?token=5535712422EEDE492F68E27E6EA2DF151BFC2E893CE21138A9E4C95B6D2738E061206D95C2DACA5284CC07DD0EF7FFBC&originRegion=eu-west-1&originCreation=20220514120411

Coleman, H. W., & Steele, W. G. (2018). *Experimentation, validation, and uncertainty analysis for engineers*. John Wiley & Sons.

Crowther, W., & Potts, J. (2007). Simulation of a spinstabilised sports disc. *Sports Engineering*, *10*(1), 3-21. : https://www.researchgate.net/publication/225330184

Discs, I. ((n.d.), March 7, 2022). *FLIGHT RATING SYSTEMS*. Innova Discs. https://www.innovadiscs.com/home/disc-golf-faq/flight-ratings-system/

Douglas Brown, W. C., Robert M Hanson. (2022). *Tracker*. In (Version 6.0.8) https://physlets.org/tracker/

Giljarhus, K. E. T. (2022). Disc golf trajectory modelling combining computional fluid dynamics and rigid body dynamics. *Sports Engineering*, *Submitted*(Submitted), Submitted. Submitted

Hubbard, M., & Hummel, S. (2000, (n.d.)). Simulation of Frisbee flight. 5th Conference on Mathematics and Computers in Sport, University of Technology, Sydney

Hummel, S., & Hubbard, M. (2002, (n.d.)). Identification of Frisbee aerodynamic coefficients using flight data. 4th International Conference on the Engineering of Sport, Kyoto, Japan.

Hummel, S. A. (2003). *Frisbee flight simulation and throw biomechanics* [Master's thesis, University of California, Davis].

Kamaruddin, N. M. (2011). *Dynamics and Performance of Flying Discs* [Doctoral thesis, University of Manchester].

Koyanagi, R., & Ohgi, Y. (2010). Measurement of kinematics of a flying disc using an accelerometer. *Procedia Engineering*, *2*(2), 3411-3416. https://www.sciencedirect.com/science/article/pii/S1877705810004200?via%3Dihub

Latitude-64. (2020, November 19, 2020). *How a Disc Golf Disc is made*. YouTube. https://www.youtube.com/watch?v=Tkr5W90hXnQ&ab_channel=Latitude64

Lee, J., Lee, Y. J., Sung, S. K., & Kim, K. (2017, June 5-9, 2017). A Novel Flight Coefficient Estimation of Flying Disc and its Performance Analysis via Onboard Magnetometer Measurement. 33rd AIAA Aerodynamic Measurement Technology and Ground Testing Conference, Denver, Colorado.

Norton, M. (2017). *Tuesday Tips: How Disc Stability And Release Angles Work Together* [Angle of release]. Ultiworld disc golf. https://discgolf.ultiworld.com/2017/05/02/tuesday-tips-disc-stability-release-angles-work-together/

PDGA. (2021, February 22, 2022). *2020 PDGA & DISC GOLF YEAR-END DEMOGRAPHICS*. Professional Disc Golf Association. https://www.pdga.com/files/pdga_2020_demographics_0_0.pdf

Tjelmeland, H. (2017, July 24, 2017). *Forventningsverdi og varians*. NTNU. https://wiki.math.ntnu.no/tma4245/tema/begreper/expectation

Young, H. D. (1962). *Statistical treatment of experimental data*. McGraw-Hill Book Company, New York.

9 Appendix

Appendix A

Appendix A provides plots of the comparison between all throws and their simulation separately.

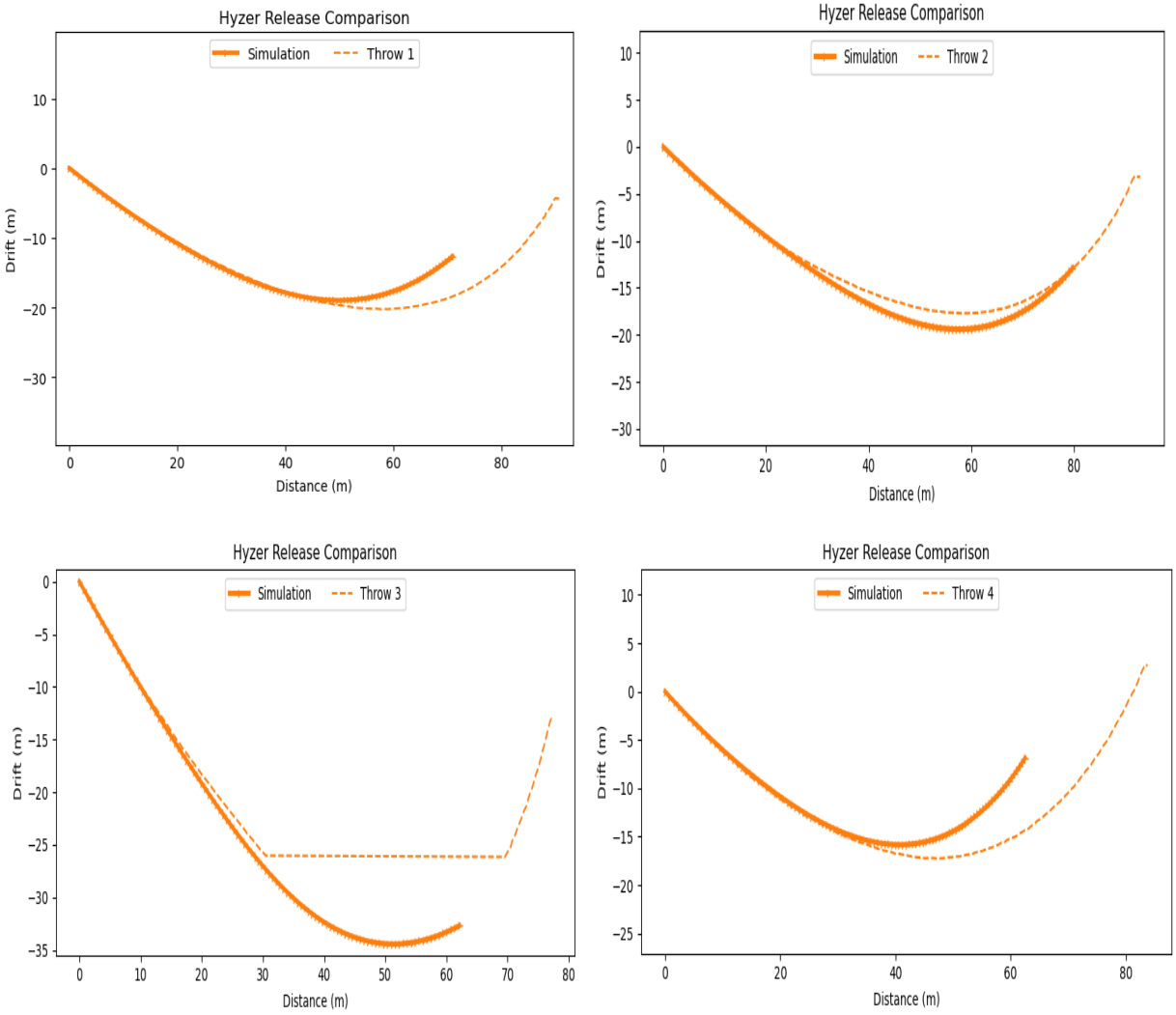

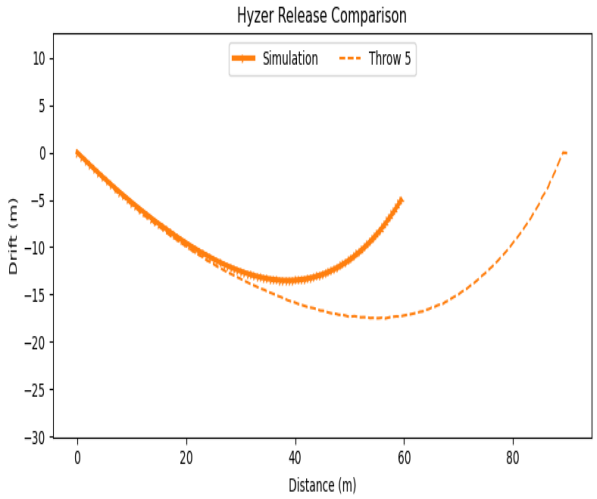
Hyzer Release Comparison
Simulation
Throw 5
Drift (m)
Distance (m)

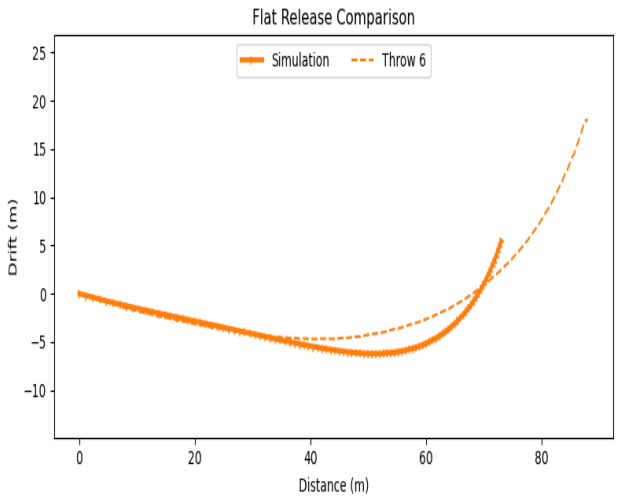
Flat Release Comparison
Simulation
Throw 6
Drift (m)
Distance (m)

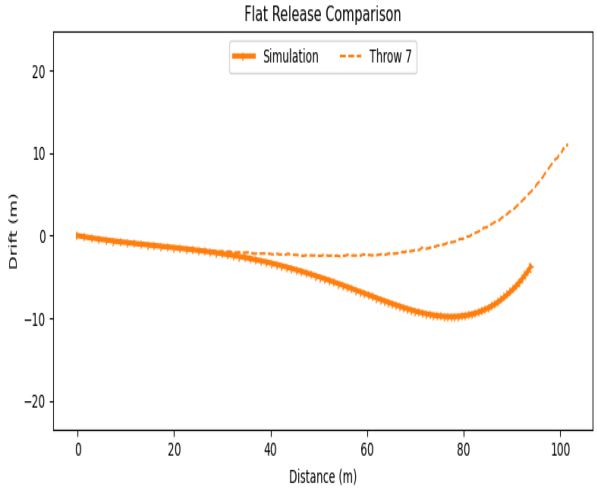
Flat Release Comparison
Simulation
Throw 7
Drift (m)
Distance (m)

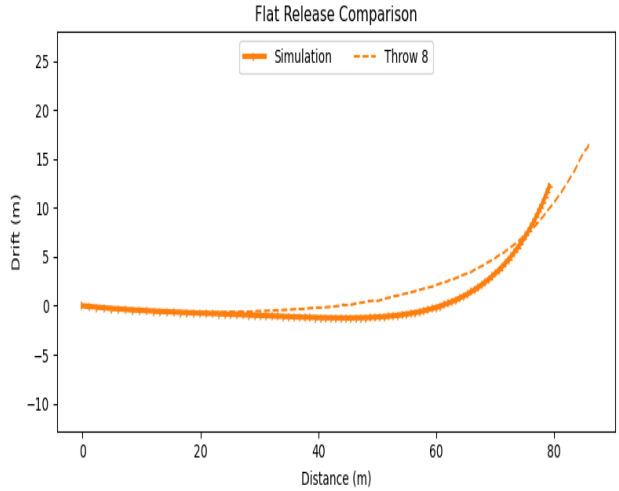
Flat Release Comparison
Simulation
Throw 8
Drift (m)
Distance (m)

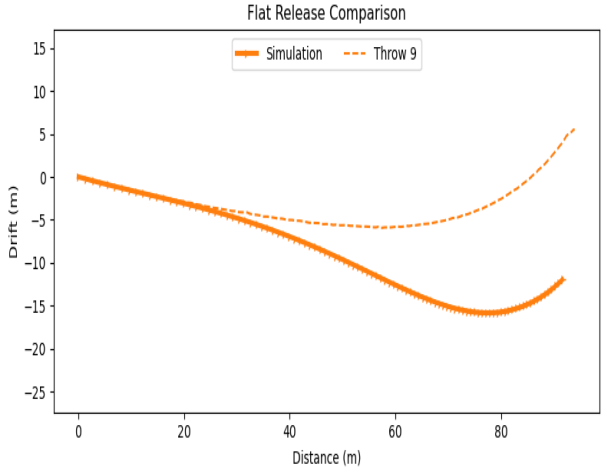
Flat Release Comparison
Simulation
Throw 9
Drift (m)
Distance (m)

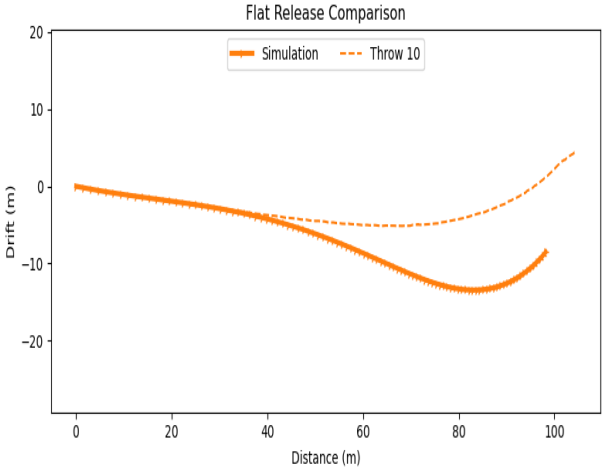
Flat Release Comparison
Simulation
Throw 10
Drift (m)
Distance (m)

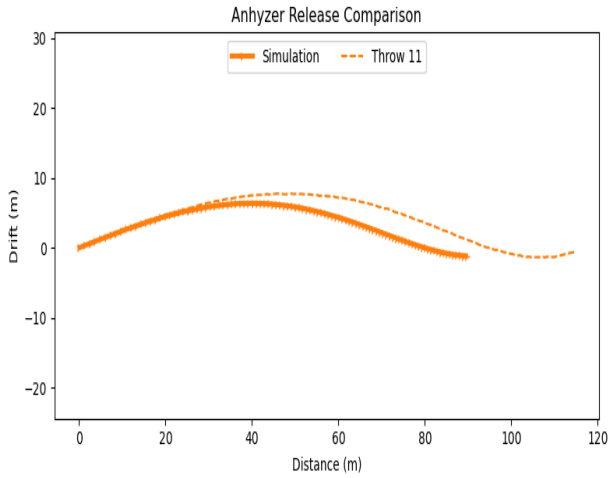
Anhyzer Release Comparison
Simulation
Throw 11
Drift (m)
Distance (m)

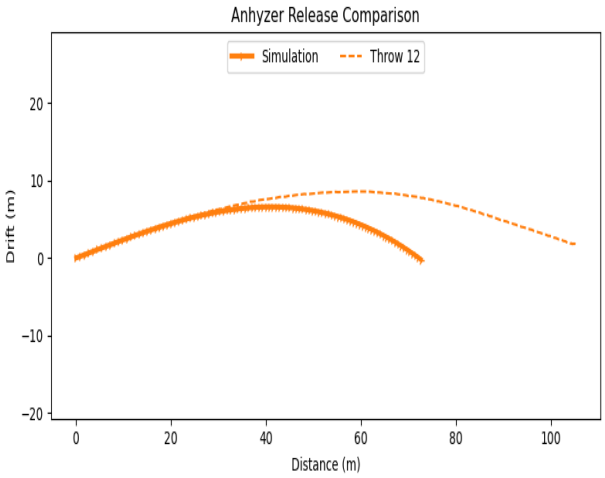
Anhyzer Release Comparison
Simulation
Throw 12
Drift (m)
Distance (m)

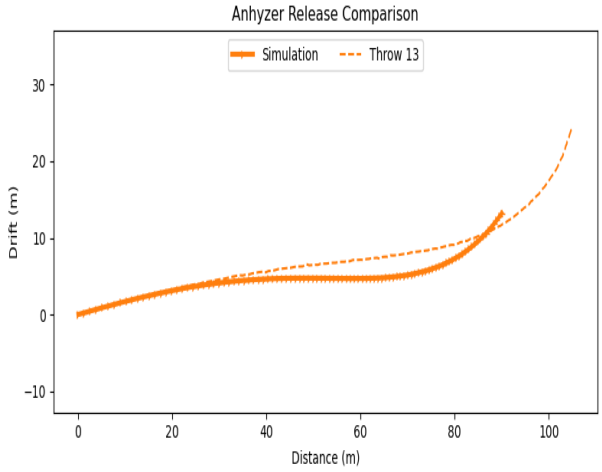
Anhyzer Release Comparison
Simulation
Throw 13
Drift (m)
Distance (m)

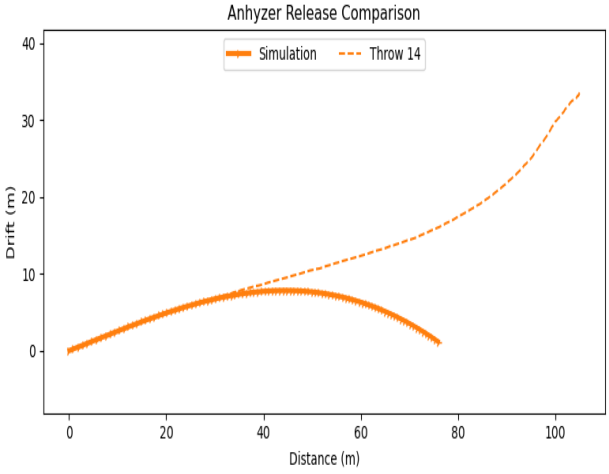
Anhyzer Release Comparison
Simulation
Throw 14
Drift (m)
Distance (m)

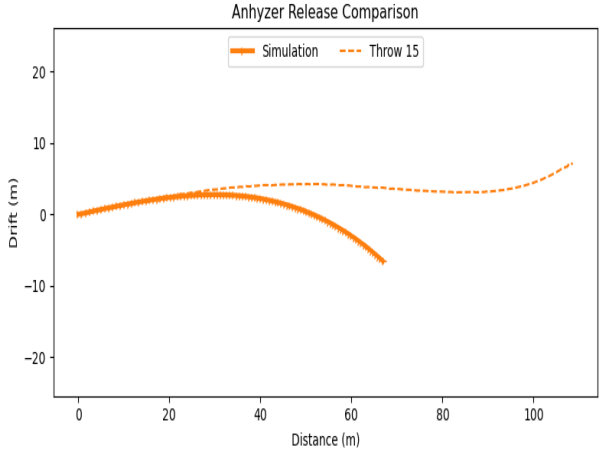
Anhyzer Release Comparison
Simulation
Throw 15
Drift (m)
Distance (m)

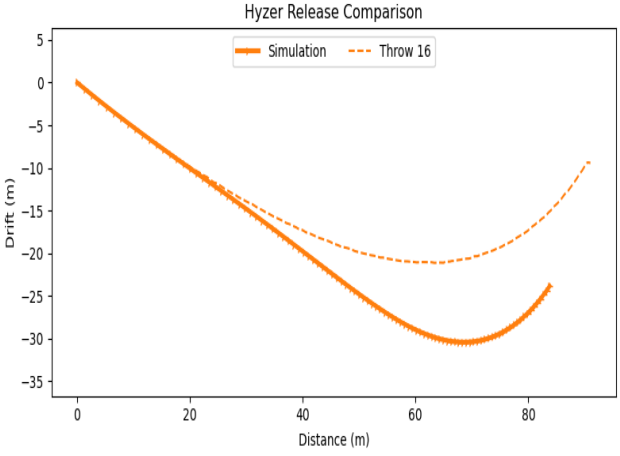
Hyzer Release Comparison
Simulation
Throw 16
Drift (m)
Distance (m)

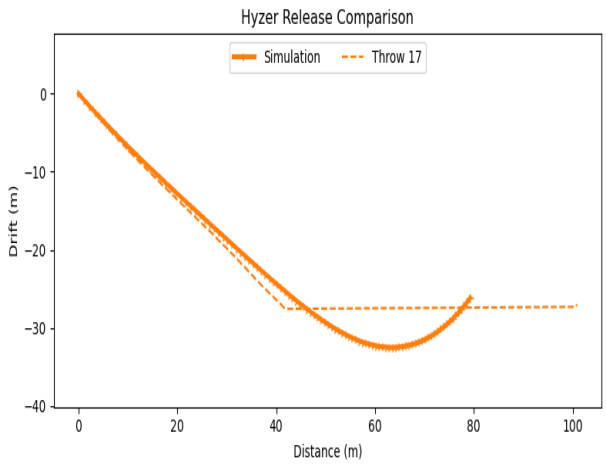
Hyzer Release Comparison
Simulation
Throw 17
Drift (m)
Distance (m)

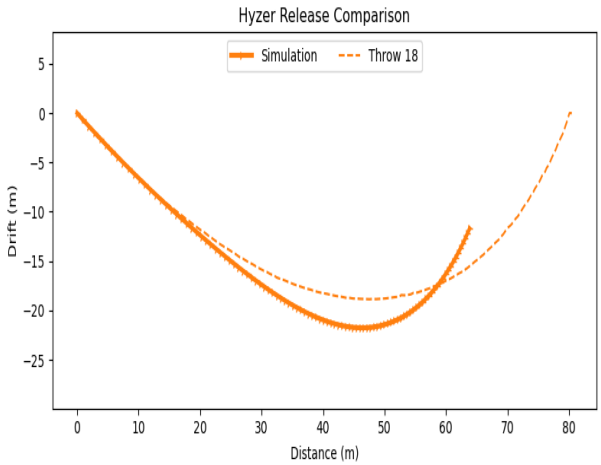
Hyzer Release Comparison
Simulation
Throw 18
Drift (m)
Distance (m)

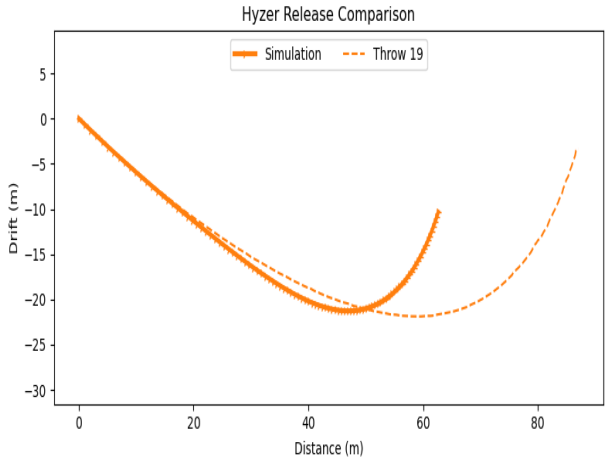
Hyzer Release Comparison
Simulation
Throw 19
Drift (m)
Distance (m)

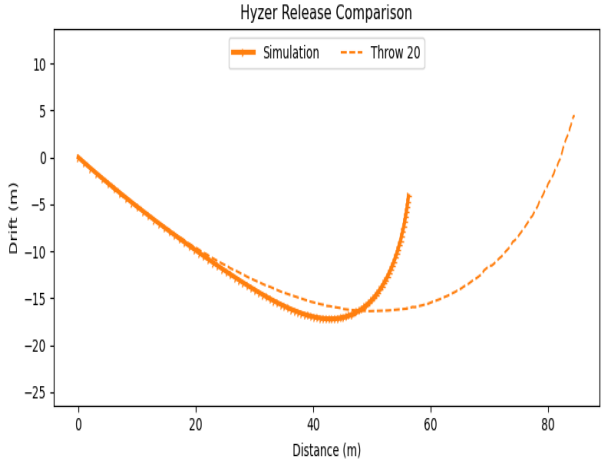
Hyzer Release Comparison
Simulation
Throw 20
Drift (m)
Distance (m)

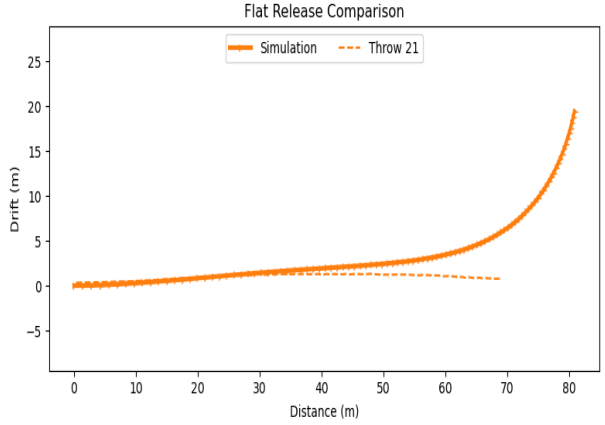
Flat Release Comparison
Simulation
Throw 21
Drift (m)
Distance (m)

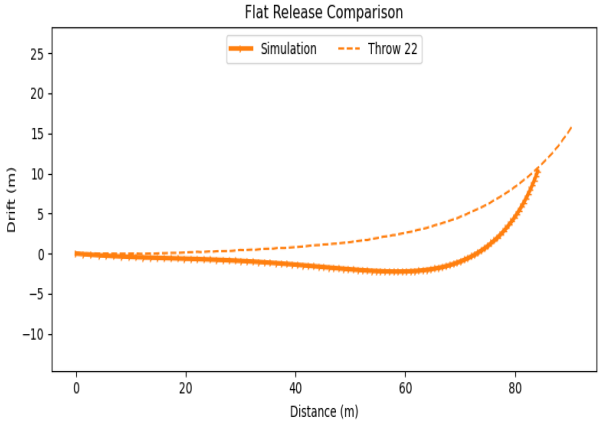
Flat Release Comparison
Simulation
Throw 22
Drift (m)
Distance (m)

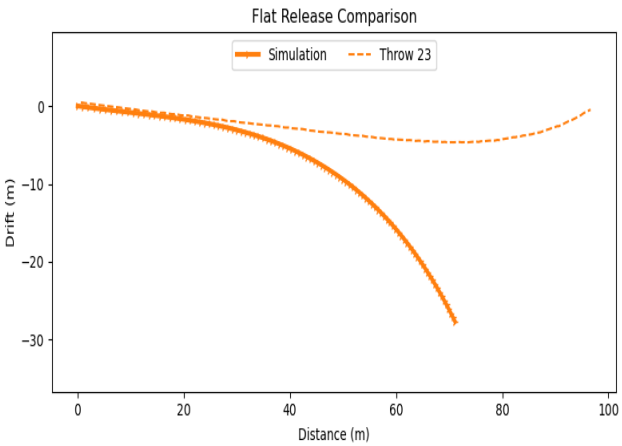
Flat Release Comparison
Simulation
Throw 23
Drift (m)
Distance (m)

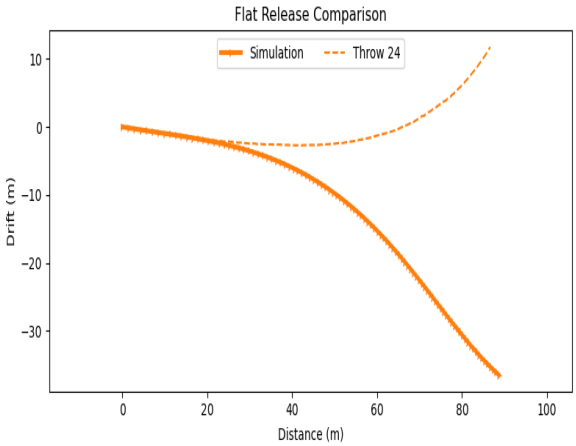
Flat Release Comparison
Simulation
Throw 24
Drift (m)
Distance (m)

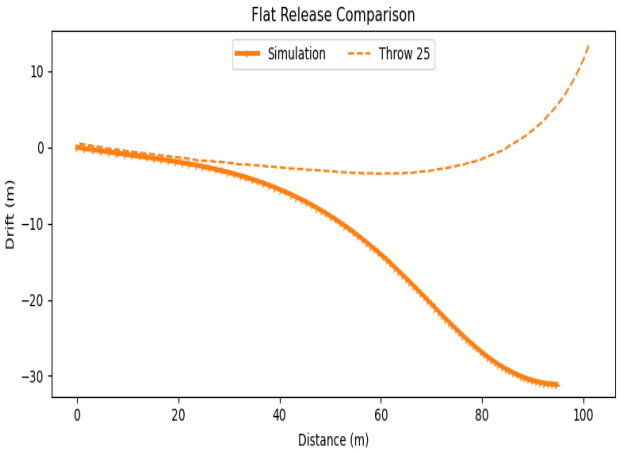
Flat Release Comparison
Simulation
Throw 25
Drift (m)
Distance (m)

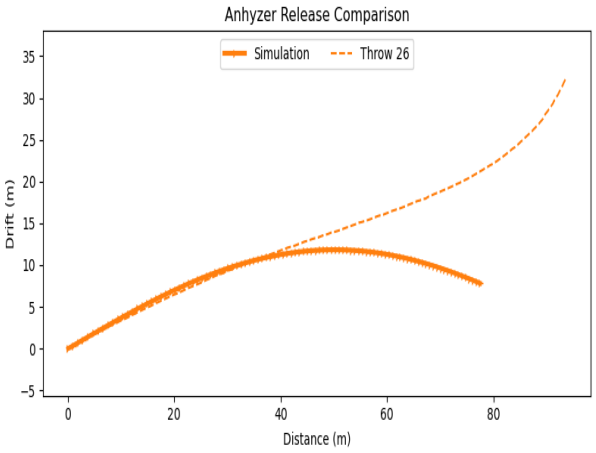
Anhyzer Release Comparison
Simulation
Throw 26
Drift (m)
Distance (m)

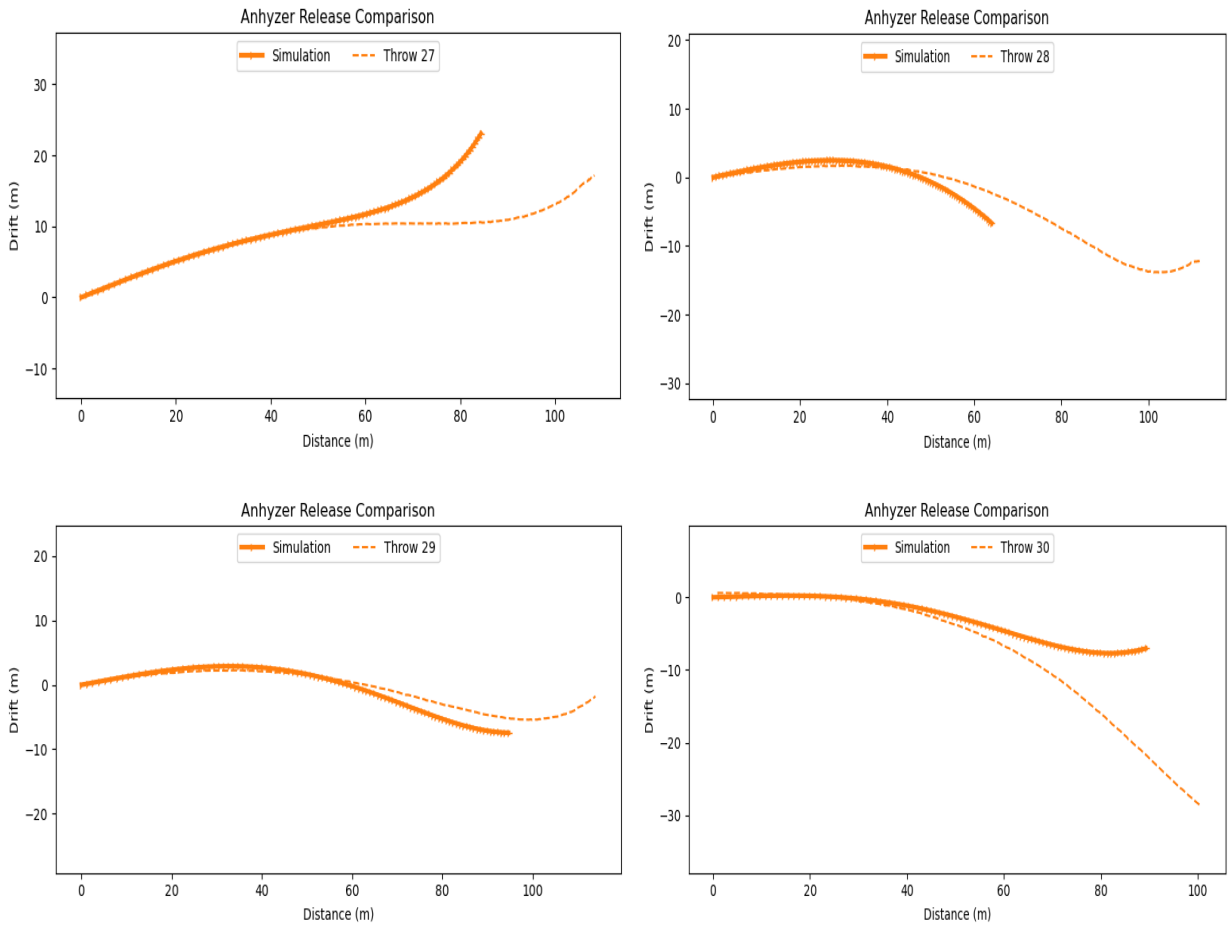

Appendix B

For the scripts used for plotting the simulated trajectories throughout this study, follow the link below:

https://github.com/kegiljarhus/shotshaper?fbclid=IwAR2l9SZgqPuKpFQbm0v9tFOja_pvsutsIa7EDx_tkzS9oOKd0YvioQXr5f8